land

MDPI

Article

Geohazard Prevention Framework: Introducing a Cumulative Index in the Context of Management and Protection of Cultural and Natural Heritage Areas

George Faidon D. Papakonstantinou * and Maria P. Papadopoulou

Laboratory of Physical Geography and Environmental Impacts, School of Rural, Surveying and Geoinformatics Engineering, National Technical University of Athens, 15780 Athens, Greece; mpapadop@mail.ntua.gr
* Correspondence: gfpapakon@mail.ntua.gr

Abstract: Geohazards pose an essential role to the preservation of cultural and natural heritage areas, given their valuable significance in terms of scenic, natural, and cultural characteristics, forming unique landscapes that require proactive action to achieve sustainable environmental management. To address these challenges, a methodological framework focusing on geohazard prevention, emphasizing the importance of a pre-management stage that enables stakeholders to prioritize resources and implement landscape planning strategies, is proposed in this paper. In this framework, an integrated set of geospatial, geological, meteorological, and other relevant environmental factors to quantify cumulative geohazard zones in heritage areas is utilized. Implementing advanced tools such as geographic information systems (GISs), remote sensing techniques, and geospatial data analysis, a clustering and characterization of various geohazards is obtained, providing a comprehensive understanding of their cumulative impacts. The introduction of a cumulative geohazard index is proposed in this paper to better understand and then assess the impacts of environmental-driven geohazards that may affect cultural and natural heritage areas to be embedded into the impact assessment process. The validation of the proposed geohazard framework and index is performed in the Parrhasian Heritage Park in Peloponnese, Greece. The outcomes of the analysis highlight the need to mitigate geohazard impacts through early and in situ targeted actions to facilitate the decision-making process and contribute to the protection of evolving landscapes with cultural and natural elements for future generations.

Keywords: geohazards assessment; protected areas management; heritage landscapes; visual resources protection; geohazard factor analysis

check for updates

Citation: Papakonstantinou, G.F.D.; Papadopoulou, M.P. Geohazard Prevention Framework: Introducing a Cumulative Index in the Context of Management and Protection of Cultural and Natural Heritage Areas. *Land* **2024**, *13*, 1239. https://doi.org/10.3390/land13081239

Academic Editors: Richard Smardon and Brent Chamberlain

Received: 28 June 2024
Revised: 29 July 2024
Accepted: 6 August 2024
Published: 8 August 2024

Copyright: © 2024 by the authors. Licensee MDPI, Basel, Switzerland. This article is an open access article distributed under the terms and conditions of the Creative Commons Attribution (CC BY) license (https://creativecommons.org/licenses/by/4.0/).

1. Introduction

This study focuses on the prevention of geological hazards that affect areas of cultural and natural heritage forming landscapes. In these areas, the objectivity of the esthetic natural and historic, archeological, and cultural characteristics describes their heritage. The combination of valuable natural and human-made features contributes to their significance and visual appeal [1]. These areas are rich in natural resources, possess exceptional beauty, are home to diverse cultures, and have a long history and traditions. It is crucial to recognize these areas as landscapes, and as landscape is a vital aspect of the environment that plays a pivotal role in spatial planning and environmentally sustainable management [2,3]. Furthermore, it is essential to recognize that these "living" landscapes are not merely objective entities but are also perceived subjectively by their users. This is particularly relevant in the context of local communities, which maintain their traditions and live within these landscapes [4,5].

Cultural and natural heritage areas comprising outstanding scenic and cultural assets form exceptional landscapes. These landscapes require protection in order to preserve their scenic, natural, and cultural treasures for future generations in a sustainable manner.

A shared understanding of vision, values, and strategies could guarantee the protection of the environment and motivate a community to work towards the preservation of the heritage identity [5]. The study of the geological evolution of such landscapes is crucial for the conservation of their cultural and natural characteristics. This process occurs over time and is influenced by various environmental factors, including the effects of climate change. In order to ensure the proper management of this evolution, it is necessary to conduct an objective evaluation.

This research concentrates on landscapes of cultural and natural heritage in terrestrial areas with mountainous characteristics due to the multitude of geological processes and environmental factors present in different regions. These processes have contributed to the formation of heritage features and continue to shape them. The valuable characteristics of heritage landscapes demonstrate that nature has generously provided its gifts in the past, which humans have used to inspire, envision, and create their myths, cultures, and lives with respect. Geology and the natural environment have been instrumental in informing people of the most suitable locations to live in for millennia. The materials used to develop their constructions, including temples and other cultural monuments, are also products of this knowledge [6]. These cultural characteristics survive to the present day. Geological history has been identified as a significant factor in the formation of these features [6]. The cultural life of the site is inextricably linked to the character and type of its natural environment. It is the physical space, with its inherent variables and unique formation, that attracts, guides, inspires, and becomes decisive in the production of the cultural trace by people. The relationship between nature and cultural heritage is direct and unambiguous. The Oracle of Delphi would not exist in its current form were it not for the specific geological characteristics of the region. The Parthenon would not have been constructed on the Acropolis if the Holy Rock had not existed. The monument and nature are in harmony with the golden ratio, as evidenced by the proportions of the Parthenon [7,8].

From the geocentric perspective, the geological processes both create and threaten this heritage, which was created years ago. These processes can affect cultural and natural heritage landscapes. While they are mainly endogenous earth processes, they interact with water, temperature, frost, or other environmental factors and occur as geological hazards, or geohazards. Landslides, subsidence, liquefaction, rockfalls, and erosion have profound effects on the cultural and natural characteristics of a site and alter landscapes [7–9]. In the context of sustainable management aimed at preserving cultural continuity and protecting natural beauty, it is essential to systematically observe the geological architecture and history of the area in order to prevent, reduce, and deter geohazards. It is of the utmost importance that cultural and natural heritage sites receive appropriate action during the pre-management stage in order to preserve their sensitive and significant features for future generations [10].

A review of the international literature on the assessment of geological hazards reveals a multitude of similar research projects [10–12]. These studies tend to focus on the assessment of a specific geological hazard, such as landslides or earthquakes, which are known to cause disasters [13–16]. However, the present research adopts a cumulative approach to assessing all geohazards that threaten cultural and natural heritage sites.

The present study addresses the prevention of geohazards that may alter cultural and natural heritage landscapes in order to avoid natural disasters. The main difference between geohazards and disasters is their respective focus and timing. Geohazard prevention entails the implementation of proactive measures designed to identify, assess, mitigate, and avoid potential geohazards before they occur or escalate into disasters. This encompasses a range of actions, including the implementation of assessments, the establishment of monitoring systems, the adoption of land-use planning strategies, and the use of structural or non-structural mitigation measures with the objective of reducing the likelihood or severity of geohazards.

This research focuses on assessment and, in particular, on a cumulative assessment approach for the prevention of all geohazards in an area due to the sensitivity of threatened heritage features. The fundamental principle of the cumulative approach is to assess the impact of all geohazards that are additive or interactive. The additive and interactive effects of geohazards can be repeated over time and distributed over space, and thus they should be "calculated" as a result of changes caused by past, present, and reasonably foreseeable future actions. It is necessary to address a cumulative geological perspective [11,17].

In this paper, a geospatial, integrated geohazard-driven methodological framework for prevention emphasizing the importance of a pre-management stage that enables stakeholders to prioritize resources and implement landscape planning strategies is proposed. This framework introduces a cumulative index to assess the potential impacts on cultural and natural heritage landscapes of terrestrial land. It consists of six functions that are linked in a loop to show the process of continuous improvement and is based on GIS technology. The framework employs a range of tools, methods, and techniques to identify geohazard zones of graded importance and specific locations within them with spatial indications for the prevention and preservation of cultural and natural heritage landscapes. The framework is implemented in the mountainous area of the Parrhasian Heritage Park (PHP), situated on the western side of the central Peloponnese in Greece. The park's landscape comprises a combination of significant cultural and valuable scenic features.

2. The Geohazard-Driven Framework and the Cumulative Index

2.1. Geohazards and Environmental Factors

The proposed geohazard-driven framework and the cumulative index have the potential to contribute to the prevention of evolving landscapes through the implementation of early actions of sustainable management and, should the necessity arise, in situ studies. In order to achieve this, it is essential to understand and assess the impacts of the cumulative geohazards through advanced methodologies and data analysis, as proposed in this study. By addressing these threats, work is contributed to the preservation of these invaluable landscapes and their associated heritage treasures for future generations.

This study first identifies the geohazards (GHs) that pose the greatest threat to the sensitive cultural and natural heritage landscapes under consideration. It then describes for each physical variable (geological characteristics, relief, soil, climate, water, and flora) the environmental factors (F_j) that contribute to the occurrence of each geohazard as follows:

(a) Landslides (GH_1), defined as the downslope movement of rock, soil, and debris, can rapidly and destructively alter terrain, posing a significant threat to human infrastructure and the preservation of unique landscapes of cultural and natural heritage.
(b) Earthquakes (GH_2) caused by tectonic activity have the potential to cause severe ground shaking, surface ruptures, and ground displacements that threaten the structural integrity of cultural monuments and buildings, resulting in irreversible damage and loss of historical artifacts.
(c) Gradual process of weathering (GH_3), influenced by atmospheric conditions, affects the physical and chemical properties of rocks and materials over time, contributing to the deterioration of cultural structures, sculptures, and architectural elements in heritage areas.
(d) Erosion (GH_4), whether caused by water or other environmental factors, represents a persistent threat to the integrity of landscapes, potentially degrading archeological sites, cultural features, and valuable geological formations.
(e) Subsidence (GH_5), which is the gradual lowering or settling of the earth's surface, whether due to natural processes or human activity, can lead to structural instability affecting buildings, monuments, and landscapes in cultural and natural heritage areas. This poses a long-term threat to the preservation of historic sites and contributes to the alteration of topographical features (Figure 1).

GEOHAZARDS (GH_i)	ENVIRONMENTAL FACTORS (F_j)					
	Geology	**Relief**	**Soil**	**Climate**	**Water**	**Flora**
Landslide	Tectonic Structures (Faults, Folds)	Slope	Lithology (Soil types)	Rainfall		
	Lithology (Geological formations)	Aspect			Hydrographic Network	Vegetation Density
	PGA (Peak Ground Acceleration)	Curvature (Slope)				
		Road Network				
Earthquake	Volcanic Activity					
	Tectonic Structures (Faults, Folds)					
	PGA (Peak Ground Acceleration)					
Weathering	Lithology (Geological formations)		Lithology (Soil types)	Land Surface Temperature		Vegetation Density
				Rainfall		
Erosion	Lithology (Geological	Slope	Lithology (Soil types)	Rainfall	Hydrographic Network	Vegetation Density
Subsidence	Lithology (Geological formations)	Topographical Wetness	Lithology (Soil types)		Groundwater	
	Tectonic Structures (Faults, Folds)	Aspect	Land Uses		Hydrographic Network	Vegetation Density
		Elevation				
		Curvature				
		Slope				
		Road Network				

Figure 1. Geohazards and environmental factors grouped per physical environmental variable.

Landslides are influenced by a combination of environmental factors that contribute to the destabilization of slopes. These factors include tectonic structures, lithology, peak ground acceleration (PGA), slope steepness, aspect, slope curvature, rainfall patterns, proximity to rivers, vegetation density, and the presence of roads [12]. These factors play a pivotal role in determining the susceptibility of an area to landslides. The geological stability of an area is influenced by tectonic structures and lithology, while the physical conditions conducive to landslide occurrence are shaped by slope characteristics and environmental cover [13–15,18–24].

Earthquakes, which are primarily driven by tectonic activity, are influenced by several environmental factors such as the presence of volcanic activity, tectonic structures, and peak ground acceleration (PGA) that are key indicators of the seismic hazard of a region [16,25–27]. The geological setting, including active fault lines and the historical occurrence of earthquakes, plays a pivotal role in the assessment of seismic vulnerability.

The process of weathering, which is the gradual breakdown of rocks due to various environmental processes, is influenced by a number of specific factors such as lithology, Land Surface Temperature, and vegetation density [28–30]. The composition of the rock (lithology) affects the susceptibility to weathering, while temperature and vegetation cover influence the rate at which these weathering processes occur.

Erosion, the process of wearing away the earth's surface, is mainly influenced by lithology, slope, rainfall intensity, proximity to rivers, and vegetation density. The type of rock (lithology) influences the resistance of an area to erosion, while slope, rainfall patterns, rivers, and vegetation cover contribute to the susceptibility of an area to erosion [16,24–34].

Subsidence, the sinking or settling of the earth's surface, is influenced by the geological composition (lithology) that plays a role in subsidence potential, while factors such as land use and groundwater conditions can exacerbate the settling of the earth's surface. It is therefore essential to understand these factors in order to assess and manage subsidence risks in a given area [35–38].

2.2. The Framework

The proposed methodological framework is based on a newly introduced index, the Geohazards Prevention Index (GPI), which is used to calculate the geohazard assessment. Additionally, a novel hypothesis is presented that distinguishes this index from current efforts to assess geohazards. To identify potentially hazardous situations, it is necessary to assess all geohazards simultaneously, spatially, and cumulatively [39].

The framework follows an iterative process comprised of six distinct functions. Each function performs internal processes and transmits the results to the next. Each iteration is concluded with the final function, which feeds new data to the next one. The interrelationships between the functions are illustrated in Figure 2.

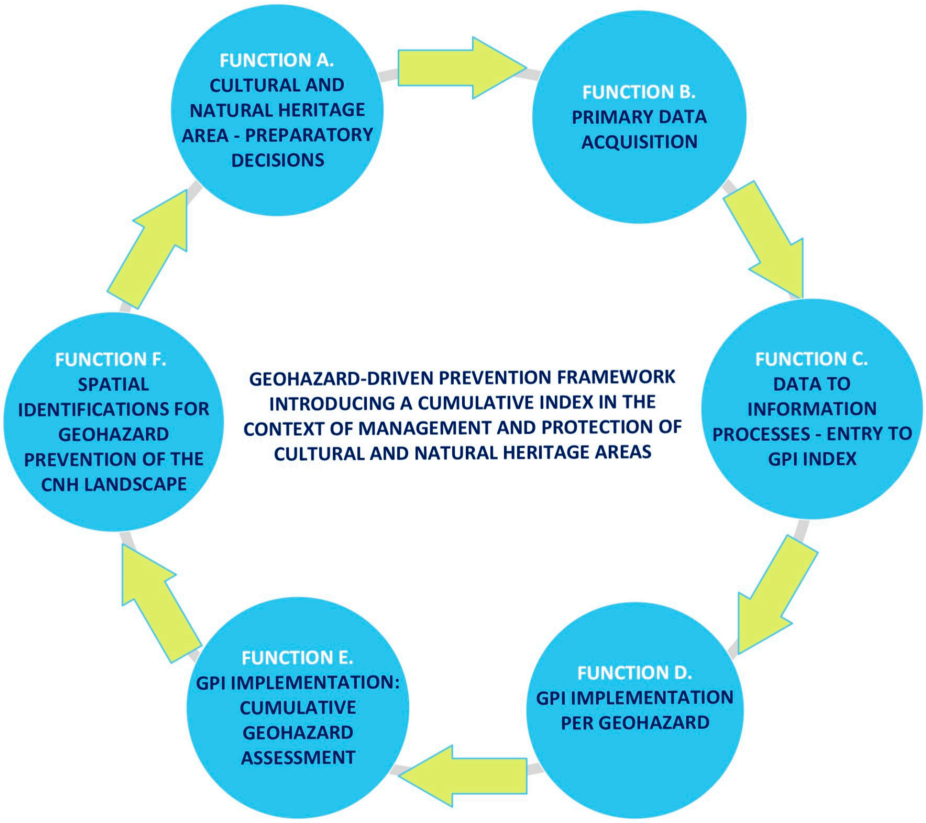

Figure 2. The methodological framework.

The initial function of the methodological framework is Function A. This is responsible for the pivotal decisions that determine the success of the geohazard assessment. Function B is informed by the outcomes of Function A. The necessary data for each identified geohazard and its corresponding environmental factors are collected. The objective is to obtain digital open-data that are available, either from the state and its archival records, from the site management units, or from the utilization of advances in technology. Remote sensing data are particularly useful for rapidly applying the GPI and obtaining prompt results. The same applies to recording cultural and natural heritage features.

Function C is responsible for the conversion of primary collected data into information, with the objective of activating the GPI. In this phase, the requisite digital layers of information are prepared for input into a geographic information system (GIS) platform.

Subsequently, the framework proceeds to Function D, during which the GPI is applied to each geohazard as defined in Section 2.1. The contribution (participation weights, w_j) of each environmental factor, F, is calculated, and geohazard maps are generated for each geohazard, GH, according to the zoning criteria.

All of the elements necessary to implement the GPI for calculating the cumulative geohazard are now available in Function E. The index will be used to calculate the cumulative geohazard. The participation weights for each geohazard in the GPI will be recalculated, and the index will be applied in total. Subsequently, a map of cumulative geohazard zones of graded importance will be generated. The map will then be subjected to a reliability check.

In Function F, a final map identifies the locations of heritage features within each graded geohazard zone. The aim is to indicate those features requiring early prevention and intervention through specific actions and field studies.

The frequency of application of the methodological framework is determined by the body responsible for managing the cultural and natural heritage area. In addition, it is essentially determined by the variation in data relating to the environmental factors that affect geohazards. After an extreme event, such as a strong rainfall event, the framework and the cumulative GPI should be recalculated.

2.2.1. Function A

The implementation of the framework commences with the activation of Function A (Figure 3), where preparatory key decisions will be made pertaining to the cultural and natural heritage area. This is a pivotal phase, as the decisions made at this point will determine the quality of the final outcome. The decisions in question concern, on the one hand, spatial definitions and, on the other hand, the definition of the content of the required information.

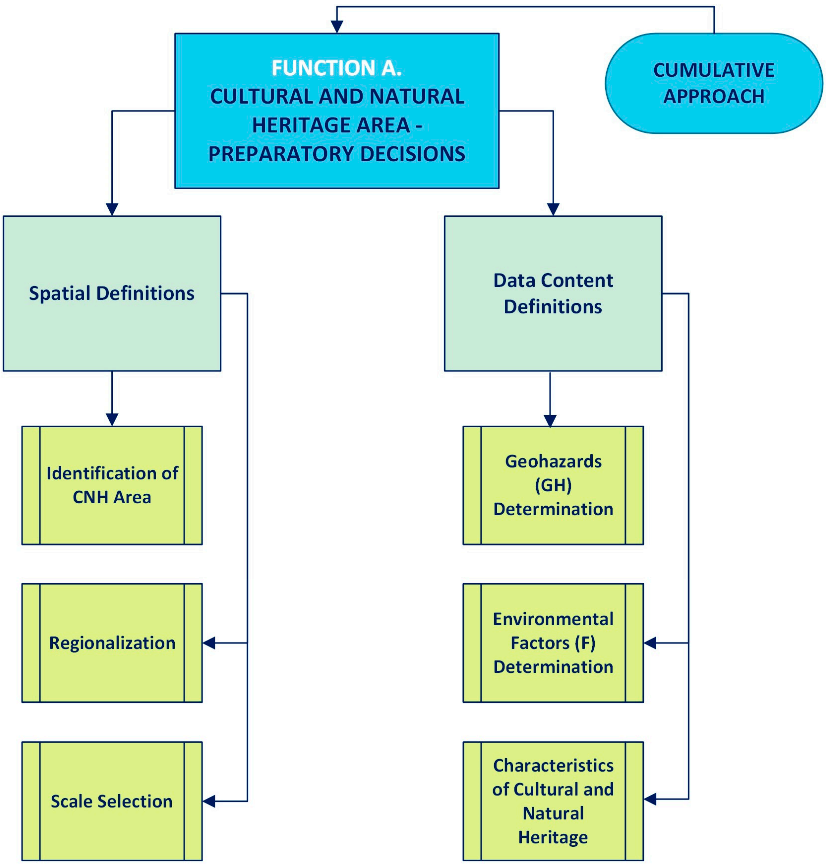

Figure 3. Cultural and natural heritage area—preparatory decisions.

Subsequently, as space is continuous and the boundaries are artificial lines, zones are defined that include adjacent areas of the boundary. This is carried out in order to ensure that critical variables that extend beyond the artificial boundaries, such as flora or fauna habitats, are studied. The area of interest is then regionalized into geographically homogeneous areas. Finally, the scale at which the primary data will be collected, attributed, and presented is determined.

As this is a cumulative approach, determining the content of the required information is of the utmost importance to ensure continuity and, above all, accuracy. For this reason, only the geohazards to be included in the cumulative index model (referred to as GH in the GPI) are identified. For each geohazard, the environmental factors contributing to its occurrence (F in the index) are identified [40]. Finally, it is important to accurately identify the cultural and natural heritage characteristics of the area in the content definition.

2.2.2. Function B

The initial data collection phase, designated as Function B, represents the fundamental stage of the geohazard assessment process (Figure 4). This stage entails the collection and compilation of primary data derived from multitude sources, including digital databases, remote sensing imagery, and archival records. The scope of data acquisition encompasses a comprehensive array of environmental factors essential for evaluating geohazard susceptibility and risk.

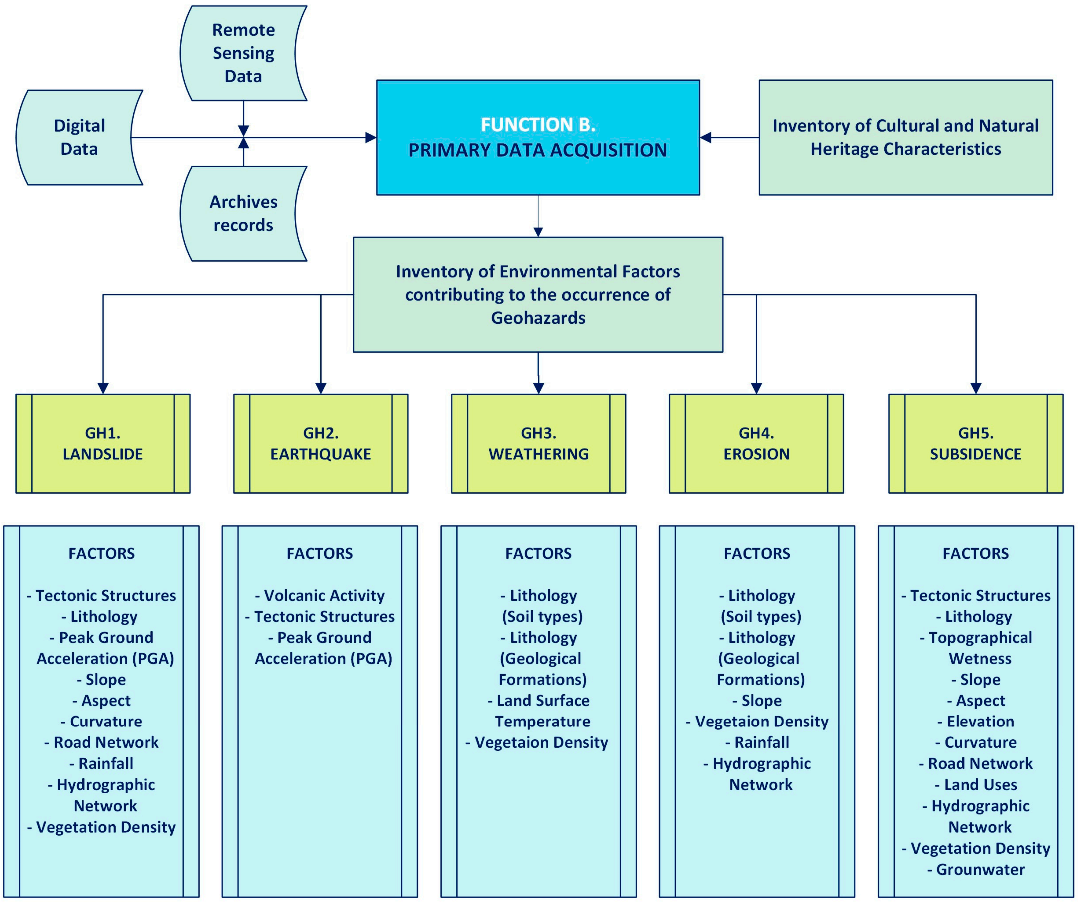

Figure 4. Primary data acquisition.

The principal datasets encompass data pertaining to geological attributes, including fault distributions, lithological compositions, and peak ground acceleration (PGA) values. These datasets provide insights into the underlying geological framework and seismic hazards within the area of interest.

Topographic features, including slope, aspect, curvature, elevation, and the Topographic Wetness Index (TWI), are surveyed in great detail in order to characterize the terrain morphology and assess the terrain stability. This is crucial for comprehending the potential for landslides, erosion, and subsidence. The road network dataset enables the identification of transportation infrastructure vulnerability, while land use data offer understandings into subsidence occurrence. Climate-related variables, including rainfall patterns and Land Surface Temperature (LST), are also critical indicators of weathering. Hydrological features, including river networks and groundwater resources, are evaluated to ascertain the influence of water dynamics on the susceptibility of geohazards. The Normalized Difference Vegetation Index (NDVI), which is employed to quantify vegetation density, offers insights into the health and stability of ecosystems. This information is useful in the assessment of landslides and other geohazards (e.g., erosion and subsidence).

2.2.3. Function C

The function designated as C represents the pivotal stage in the transformation of raw data into actionable information, thereby establishing the gateway to the GPI. Following the selection of pertinent factors, a systematic classification process ensues, categorizing these factors into distinct classes and rank values (Figure 5).

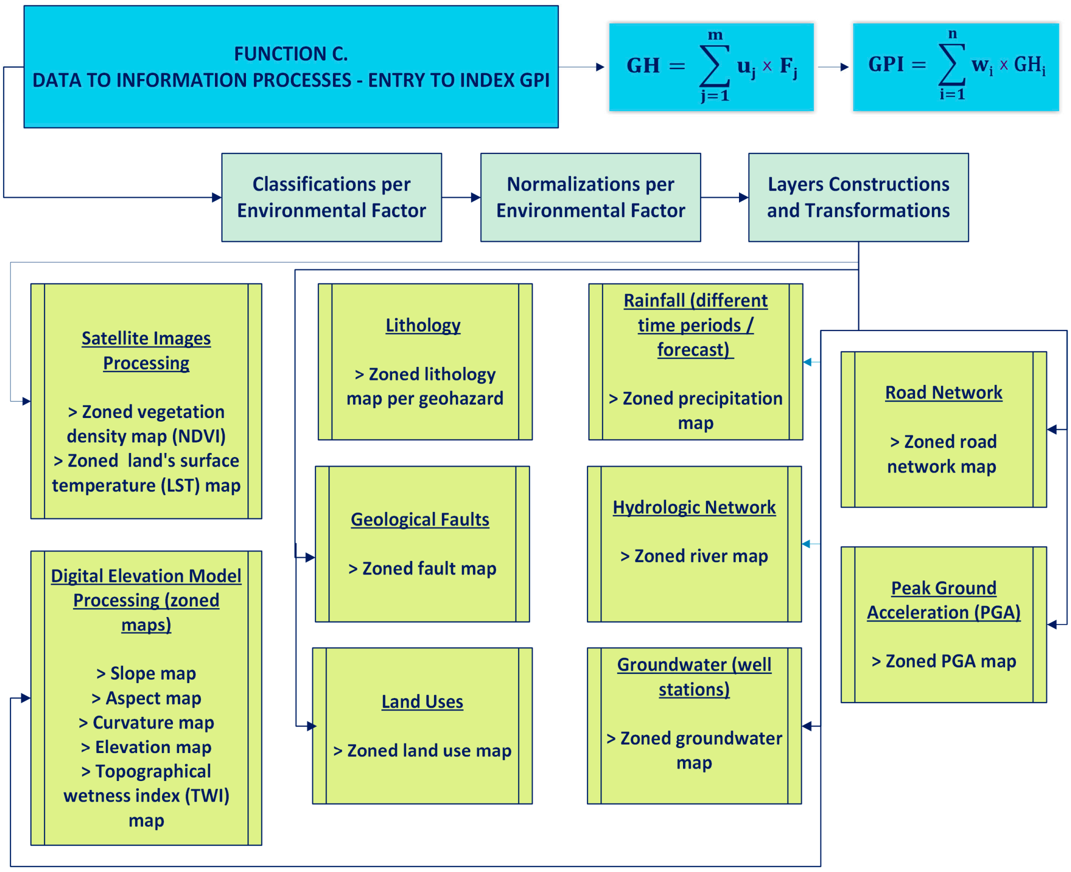

Figure 5. Data for information processes—entry for GPI.

In order to facilitate meaningful comparisons and analyses, each class is assigned a crafted set of standardized ratings. This standardization is achieved through the application of robust statistical methods, including the calculation of the z-score expressed by Formula (1).

$$z - score = \frac{x - xmin}{xmax - xmin} \tag{1}$$

The application of these methodologies ensures that the inherent variability within each factor is normalized, thereby providing a consistent and equitable basis for assessing geohazard potential across different parameters. This harmonization process establishes the foundation for subsequent aggregation of factors within the GPI, thereby providing a comprehensive framework for evaluating cumulative geohazard risk within the CNH area.

In addition, the use of geographic information system (GIS) software (QGIS Desktop version 3.28.11) enabled the generation of distinct layers for each factor, thereby enhancing the analytical capabilities of the study. The utilization of Landsat 8 satellite imagery enabled the generation of zoned map layers for vegetation density (NDVI) and Land Surface Temperature. These layers offered understandings into the dynamics of flora and thermal variations across the area of interest.

The utilization of digital elevation models (DEM) enabled the creation of additional zoned map layers, which delineated the terrain characteristics. These encompassed zoned maps for slope, aspect, curvature, elevation, and the Topographic Wetness Index, providing detailed representations of the topographic features that are crucial for the assessment of terrain stability and vulnerability to geohazard events.

Moreover, zoned map layers were developed for lithology, faults, land uses, peak ground acceleration, rainfall distribution, rivers, groundwater, and road networks. Each of these layers provides essential spatial data pertinent to geohazard assessment. These layers serve as foundational datasets for subsequent analyses, facilitating the integration of diverse environmental factors into the GPI (Formula (2)).

The final cumulative geohazard GPI, which may be caused in the cultural and natural heritage site by n identified geohazards, is the sum of the calculated hazard of each geohazard (GHi), where i = 1 to n, expressed in terms of the total geohazard with the significance of the contribution of each geohazard to it (i.e., multiplied by the corresponding identified weight w_i).

$$GPI = \sum_{i=1}^{n} w_i \times GH_i \tag{2}$$

Consequently, each geohazard (GH) is calculated as the sum of m environmental factors (F_j), where j = 1 to m, multiplied by the corresponding identified weight of the factor (u_j), expressed by Formula (3).

$$GH = \sum_{j=1}^{m} u_j \times F_j \tag{3}$$

2.2.4. Function D

The application of the Analytic Hierarchy Process (AHP) [41] to assign weights to each factor for individual geohazards is the fundamental aspect of Function D (Figure 6). This ensures a systematic and rigorous assessment process.

AHP is a decision-making methodology developed by Saaty in 1980 that is widely used for complex multi-criteria decision analysis problems [41]. The process involves pairwise comparison of criteria or factors based on their relative importance to a decision problem (Figure 5). The steps are as follows: structure the hierarchy; perform pairwise comparisons (use a scale to compare each pair of criteria); calculate weights (derive priority scales from the comparisons); synthesize results (combine the weights to determine the best decision); and check consistency (ensure the comparisons are consistent).

In AHP, decision-makers engage in pairwise comparisons of factors and assign subjective numerical values representing their relative importance. The pairwise comparisons are frequently conducted using a scale from 1 to 9, where each number represents a specific level of relative importance or preference (equal importance (1); weak or slight importance (3); moderate importance (5); strong importance (7); extreme importance (9); and intermediate values (2, 4, 6, 8) that are used to represent compromises between the preferences in the scale). Subsequently, the comparisons can be organized into a Pairwise

Comparison Matrix (PCM), where each element is compared with each other, including itself [41].

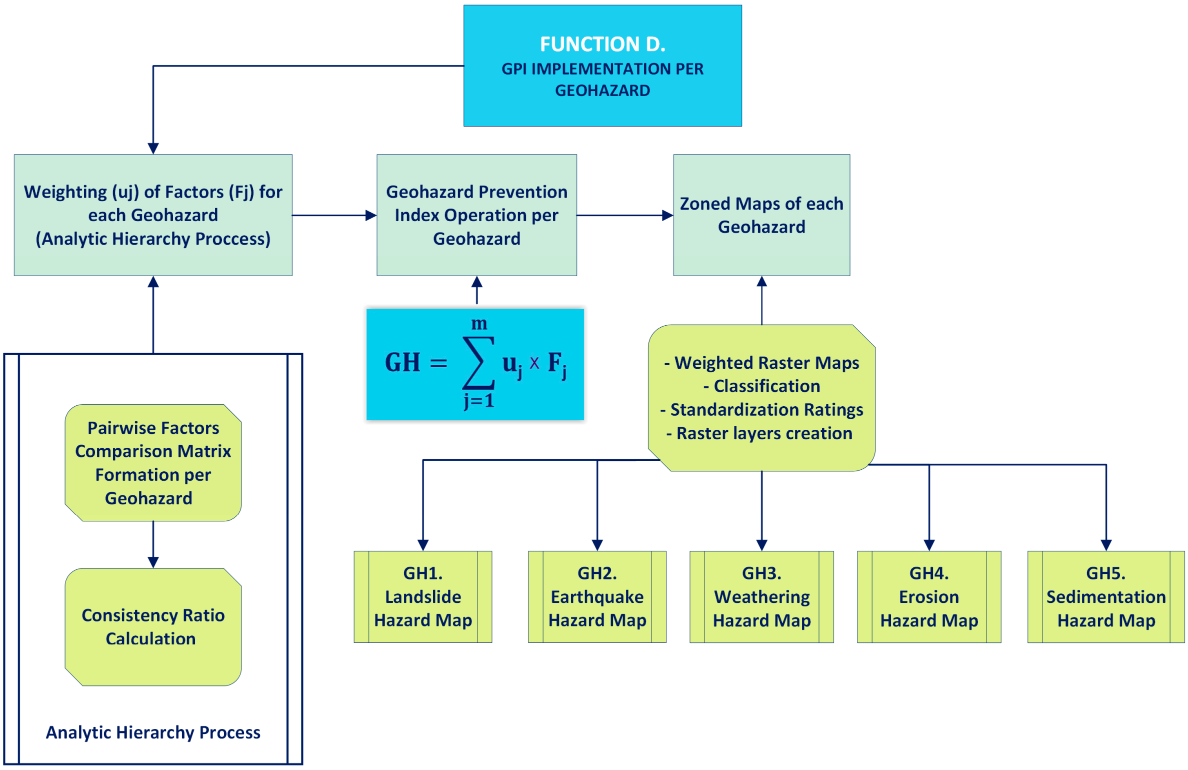

Figure 6. GPI implementation per geohazard (GH).

To ensure consistency and reliability in the pairwise comparisons, consistency ratios (CRs) are calculated for each PCM that serve to quantify the degree of agreement or consistency observed in the pairwise comparisons. Should the consistency ratio exceed a predefined threshold, typically 0.1, adjustments are made to ensure greater coherence in the comparisons [41].

Once the pairwise comparisons have been completed and consistency achieved, the Analytic Hierarchy Process yields weight vectors representing the relative importance of each factor for each geohazard. The steps after constructing the PCM are normalizing the PCM (summarizing each column and dividing each element of the matrix by the sum of its column), averaging the normalized columns, and finally dividing each sum by the number of criteria to obtain the weight vector w. These weight vectors serve as the foundation for aggregating the factors and generating weighted raster maps through the use of geographic information system (GIS) software [42].

The weighted raster maps integrate the influence of each factor on geohazard susceptibility, thereby providing a comprehensive spatial representation of geohazard potential within the area of interest. Subsequently, zoned maps of geohazards are generated by summing the weighted values of each factor and standardizing them for every geohazard. The zoned maps offer insights into the spatial distribution and severity of geohazards, thereby enabling informed decision-making and risk management strategies tailored to the specific characteristics of each hazard type and its underlying contributing factors [43].

2.2.5. Function E

In Function E, the Analytic Hierarchy Process is employed once again, this time to determine the relative importance of the different geohazards within the area of interest (Figure 7). Through pairwise comparisons, weights are assigned to each geohazard based on its perceived significance, ensuring a systematic and informed decision-making process. The reliability and coherence of the pairwise comparisons are rigorously monitored through the use of consistency ratios. Each geohazard is assigned a weight, and geographic information system (GIS) software is employed to aggregate the data, thereby creating a weighted raster map of the GPI. This index serves as a quantitative measure of the cumulative geohazard potential.

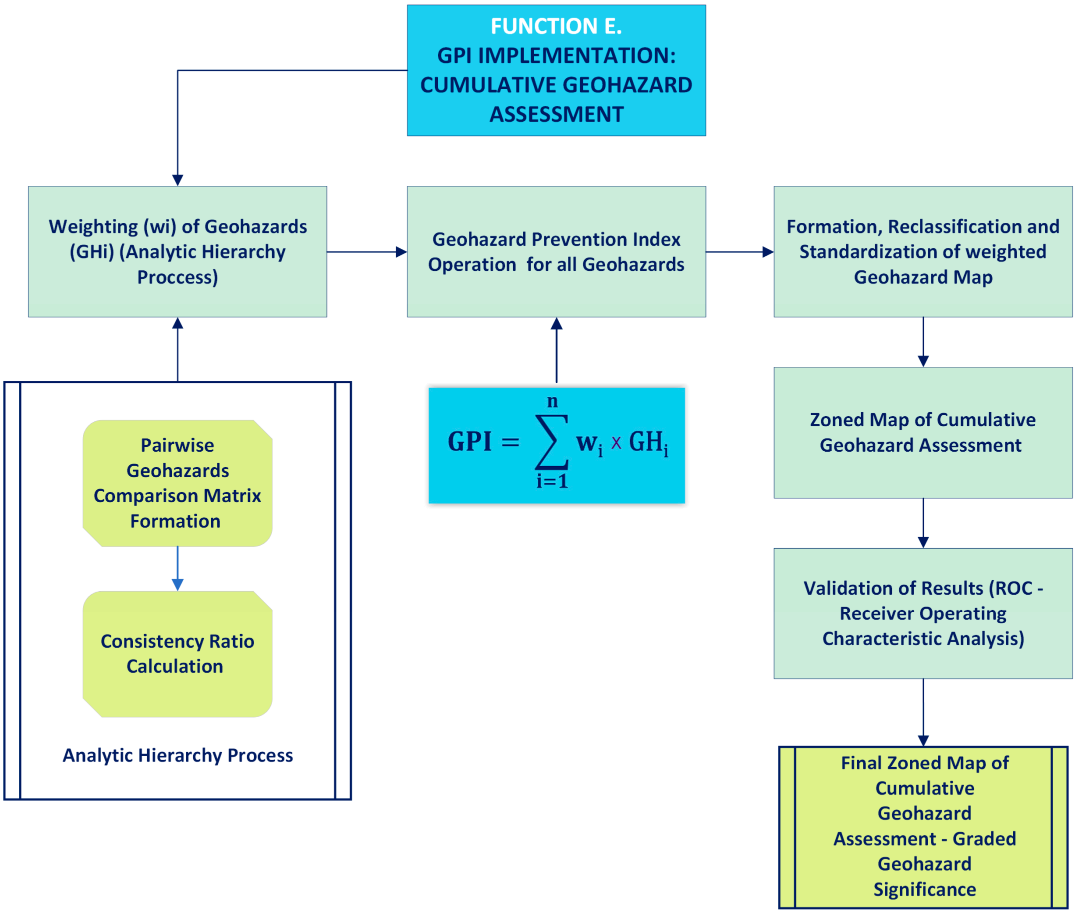

Figure 7. GPI index implementation: cumulative geohazard assessment.

Subsequently, the GPI is standardized, after which a new map is generated. The final map of the cumulative geohazard map is then generated by ranking the standardized GPI values. This process yields insights into the spatial distribution and severity of geohazard risks. To validate the accuracy and reliability of the results, a Receiver Operating Characteristic (ROC) analysis is conducted, comparing the model's predictive performance against observed geohazard occurrences [44]. The validated results are used to produce the final zoned map of the cumulative geohazard assessment, which delineates graded geohazard significance. The map provides understandings that enable targeted mitigation efforts and informed decision-making to mitigate geohazard risks and enhance overall disaster resilience.

2.2.6. Function F

Function F plays a pivotal role in the integration of the methodological framework, as illustrated in Figure 8. It establishes a spatial relationship between the final zoned map of cumulative geohazard assessment, the landscape character zones, and the cultural and natural heritage characteristics of the area of interest. The outcome of these relationships is the identification of sub-zones of notable geohazard significance for the heritage features they contain. The objective is to conserve these heritage features and, consequently, to safeguard the landscape in which they are situated. This may be achieved either by considering the cumulative impact of the geohazards present in the area or by providing detailed information on each hazard separately. The methodological framework assists planners and managers in determining the prevention indications required to mitigate geohazards over time, prevent their further evolution, and enhance the protection of heritage features. These prevention indications may take the form of specialized actions or in situ studies, depending on the significance of the geohazard and the type, detail, and context of the heritage features in question.

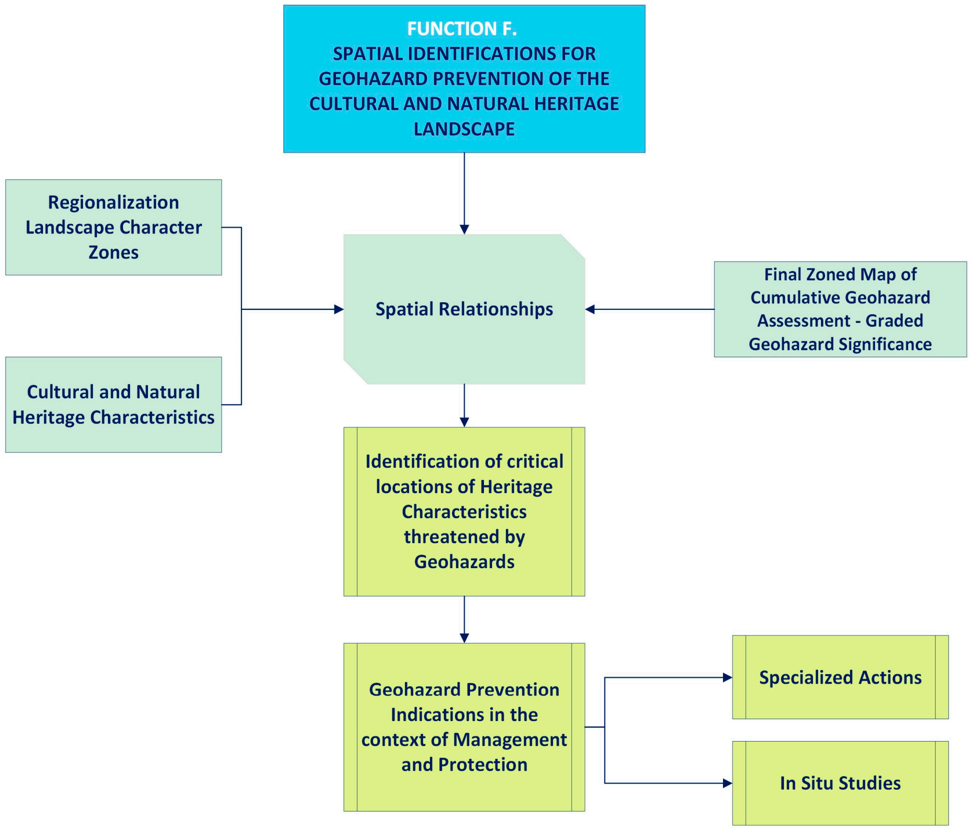

Figure 8. Spatial indications for geohazard prevention.

3. GPI-Based Framework Subject to Field Testing

3.1. The Parrhasian Heritage Park, Landscape Character Zones, and Heritage Characteristics

The implementation of the proposed GPI-based framework was carried out in the Parrhasian Heritage Park (PHP), a region situated in Peloponnese, Greece. The area is defined by its delineated boundaries, which encompass four sub-areas that have been identified as landscape character zones. These zones have been derived from a comprehensive regionalization study that has examined the rich cultural and natural heritage of the area in quest [45]. Moreover, the area is subject to geological hazards that affect it and the associated environmental factors to which each geological hazard is related.

3.1.1. The Parrhasian Heritage Park

The PHP is situated in the western part of Central Peloponnese, encompassing an area of 670 km^2. The designation of PHP is in reference to the ancient name Parrhasia, which was historically regarded as the oldest inhabited area in mainland Greece. The inhabitants of the ancient region (the Parrhassians) are referenced in Homer's Eliad, Rhapsody B. They fought on the side of the king Agamemnon in the Trojan War [46].

At the regional level of self-government, it occupies part of two regions: the Region of Peloponnese and the Region of Western Greece. The PHP comprises portions of three prefectures: Arcadia, Elis, and Messinia. Figure 9a illustrates the location of the PHP within the broader context of the Peloponnese region in Greece. Figure 9b presents a more detailed representation of the PHP [47]. The coloured areas in the picture are the landscape character zones of the PHP. The text of the image is bilingual (English and Greek translation).

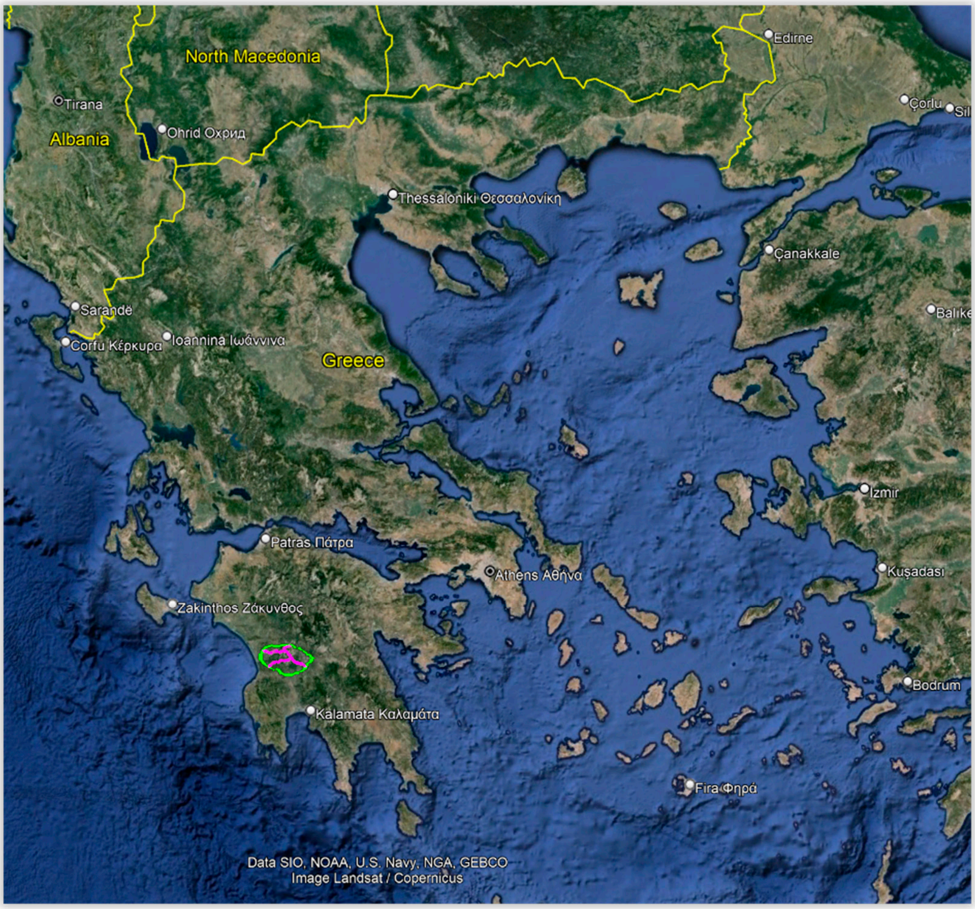

(**a**)

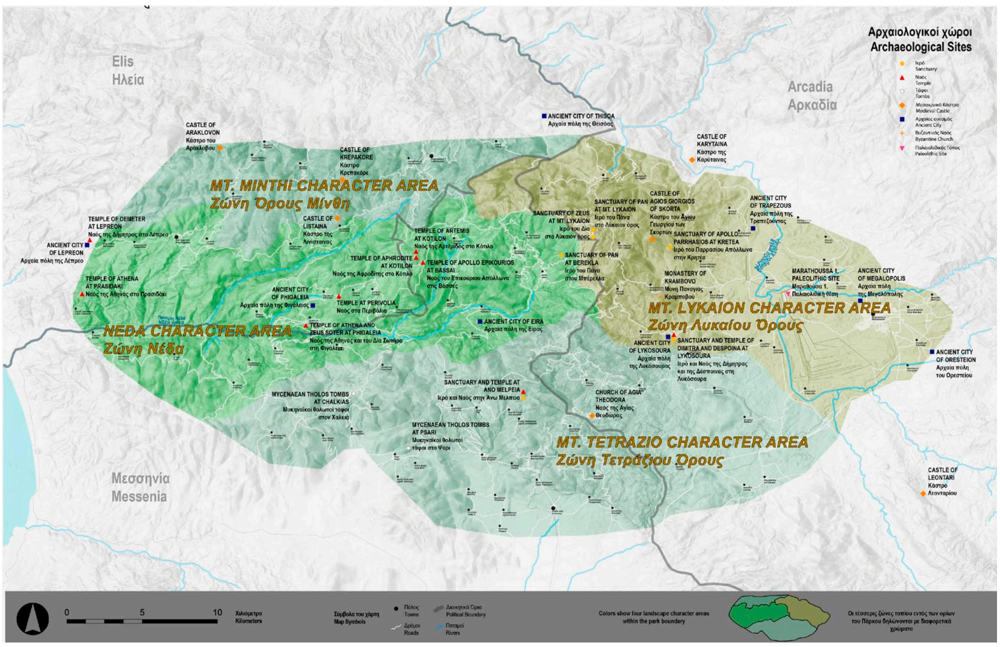

(**b**)

Figure 9. (**a**) The PHP in Greece. (**b**) The PHP in detail.

At the municipal level, the PHP consists of five municipalities. In the Peloponnese region, the PHP extends from east to west through the municipalities of Megalopolis (which occupies 37% of the PHP), Oichalia (31%), and Trifylia (7%). In the region of Western Greece, from west to east, it occupies part of the municipalities of Zacharo (14%) and Andritsaina Crestenon (about 10% of the PHP). It is noteworthy that the PHP does not include any Natura 2000 sites, although it does encompass a small portion of a wildlife sanctuary in its south–central region, namely Oichalia.

The area is distinguished by the presence of three major mountain peaks, with Mount Minti to the north, Mount Tetrazion to the south, and Mount Lykaion to the east. Mount Lykaion serves as a natural boundary between the watershed areas to the east and west. The Lykaion is the source of the springs and the surrounding mountains that feed the Neda River. This river flows from east to west through the area and ultimately empties into the Kyparissiakos Gulf [46]. The PHP is dominated by four gateway cities, which are the largest cities in the region, and each has a zone of influence around them. The gateways are located in distinct local zones of the region and are Megalopolis in Arcadia to the east, Andritsaina to the north, Nea Figalia in Elis to the west, and Diavolitsi in Messinia to the south [46].

The PHP is a geologically distinct area in the Peloponnese with significant natural and cultural characteristics that form visual resources. It has been delineated and systematically studied by a scientific team comprising members of three universities: the University of Arizona, the National Technical University of Athens, and the University of Patras, and has been proposed to be established as a protected landscape. This research collaboration has been ongoing since its inception and continues to this day [46].

3.1.2. Landscape Character Zones and Heritage Characteristics

The concept of cultural and natural heritage sites being considered landscapes is a proposition put forth in the literature. Landscapes, with their tangible and intangible dimensions, have particular natural features, prominent or particularly distinctive elements (such as particular geological formations, etc.), despite their biodiversity. These elements are the result of ecological, physical, functional, and anthropogenic relationships that reflect the characteristics of socio-economic systems [48,49]. Furthermore, landscapes have intangible relationships with their inhabitants, or with the inhabitants of wider areas, or with their visitors, which can be historical or collective in nature, symbolic, emotional, and esthetic [50]. In most cases, they form a relative "totality" that links them, united by one or more main characteristics. This unity in diversity gives the place (locus) its distinctive character, which can be described as a 'landscape' [50,51].

The research hub of the three universities identified in the PHP four landscape character zones [47,52–54]. The landscape zones of Mount Lykaion, Mount Tetrazion, Mount Minthi, and Neda comprise the final boundary of the PHP (Figure 10).

- The Minthi landscape zone, located north of the Neda River, was a site of conflict between local Greek barons and invading Frankish crusaders during the Middle Ages. It encompasses the summit of the mountain range and its steep limestone lower slopes.
- The Mount Tetrazion landscape zone is demarcated by the point where the extensive oak-covered slopes of the mountain emerge onto the plain below. It is centered around the limestone peak of Mt. Tetrazion, formerly known as Mt. Nomia, where it was believed that the god Pan had his mountain pastures.
- The landscape character zone of Mt. Lykaion is situated in a seismically active region, which has resulted in the emergence of seven springs and water sources [55,56]. The boundary for the zone is defined by Mount Lykaion and the lower slopes to the north and south of the River Alpheios, which is the longest river in the Peloponnese with a catchment area of 3700 km^2, while to the east it includes Megalopolis and its lignite mine.

- The Neda landscape zone lies at the point where the Neda River rises from the steep mountain valleys in an extraordinary gorge to its edge before the river exits into the plain.

Every August, a series of cultural events is organized by local residents throughout the PHP.

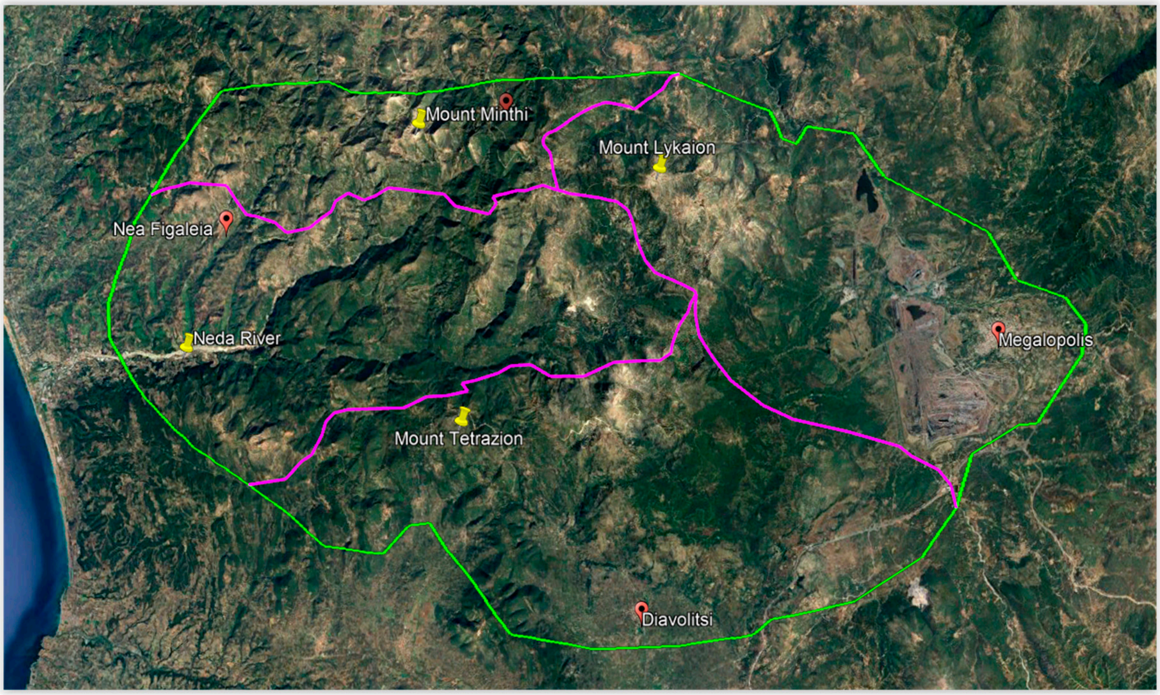

Figure 10. Landscape character zones (purple lines) with three mountain volumes and four gateway cities. Green line represents the PHP's boundary.

The Peloponnese exhibits a high degree of geological, geomorphological, and climatic variability, as evidenced by the region's diverse range of regional and local activities over time. The bedrock and typical landforms are primarily composed of Mesozoic limestone, which is the result of tectonic activity and major events such as floods, earthquakes, and river sediment deposition [55,57,58]. The result of these activities is a diverse landscape comprising a multitude of features within a relatively confined geographical area. These include mountains, limestone caves, gorges, rocky outcrops, forests, rivers, waterfalls, valleys, springs, ancient cities, sanctuaries, and picturesque villages that illustrate a rich cultural and natural history [56].

The mountains in the area were formed in an ancient ocean that existed before the Mediterranean, between 175 and 50 million years ago. The uplift of the seabed to its current height required deep faulting, which resulted in the stacking of 1000-meter-thick layers on top of each other. The erosion caused by rivers and streams in this region has been significantly influenced by fault patterns. Variations in soil types and agricultural fertility are likely to follow underlying geological patterns. Springs emerge from the fault zones, acting as natural plumbing systems to carry water through the fractured and sheared rock. Mountain villages were typically established at spring sites. In contrast to previous mountain buildings, the Peloponnese is currently undergoing a process of extension, which is similar to the more noticeable extension of Greece observed in the Gulf of Corinth [53].

The region's vegetation is highly diverse due to the long-term influence of human activity. The region's vegetation includes high alpine vegetation, mountainous coniferous forests with pine, black pine, and local fir stands, mixed deciduous forests (predominantly oak on the mountain slopes), and scrub vegetation on the exposed limestone [55].

The area's primary natural features include large, mature oak forests on the lower slopes of the mountains, as well as the peaks of Mt. Minthi and western Mt. Tetrazion, which overlook the upper course of the Neda River. This river is renowned for its dramatic waterfalls and steeply carved gorges. The forests on the south side of the Neda River are characterized by high density and lush vegetation, while on the north side they are limited to steep slopes and valleys. In other areas, the forests have been cleared for the cultivation of olives and the construction of agricultural terraces. Oak and chestnut trees are found in the upper regions along the Neda River. Additionally, oak forests are found in protected valleys, including Ampeliona, Agios Sostis, and Petra. Naturalized chestnut trees are found in mixed stands with oaks, and they also grow in isolated, unmixed stands. The cultivation of chestnuts has been encouraged by human intervention, with the resulting harvests being used to produce traditional products in the villages of the area. They are frequently cultivated on agricultural terraces where barley was previously the predominant crop [52–54].

The region is home to a plethora of valuable cultural characteristics that have evolved in parallel with the natural environment. The Park includes a number of significant archeological sites, including the ancient cities of Lykosoura and Trapezous, the sanctuaries of Zeus, Pan, Demeter, and Despoina, the only excavated hippodrome in Greece, and the Temple of Apollo Epikourios, designed by Iktinos, the architect of the Parthenon in Athens (the inaugural UNESCO World Heritage Site in Greece) [54].

3.2. Inventory of Environmental Factors and Processes for Entry to the GPI

The geological hazards selected for consideration in the PHP are landslides (GH1), earthquakes (GH2), weathering (GH3), erosion (GH4), and subsidence (GH5) (Figure 4). These hazards pose a threat to the cultural and natural heritage of the PHP [59]. They can significantly alter its landscape and have the potential to cause significant damage [60]. The environmental factors analyzed in this section are those identified in Section 2 (Figure 4).

3.2.1. Primary Data Acquisition

The primary dataset consists of the following sections 1–10: Information on the data source and the GIS data type are provided in Appendix A.

1. One of the key tools for identifying the environmental factors that contribute to geohazards is the Landsat 8 satellite image of the PHP. The satellite provides multispectral imagery with a spatial resolution of 30 m for most bands, which is particularly useful for capturing a comprehensive view of the landscape while maintaining a balance between detail and coverage. The Landsat 8 satellite acquires data in multiple spectral bands, including the visible, near-infrared, shortwave infrared, and thermal infrared. The extensive range of bands enables the extraction of valuable information on land cover, vegetation health, and surface temperature. The satellite revisits the same area every 16 days, thereby ensuring the regular and consistent collection of data. This temporal resolution is of particular importance for the monitoring of changes over time, particularly in dynamic environments that are susceptible to geohazards [17]. A satellite imagery-based analytical approach was employed within the QGIS environment to extract key environmental indicators. The Normalized Difference Vegetation Index (NDVI) was calculated to characterize vegetation density across the extensive area of study. Concurrently, the determination of Land Surface Temperature (LST) provided insight into the temperature distribution across the earth's surface. The derived indices, created through the use of geospatial techniques, provide crucial data that can be used to unravel the intricate spatial dynamics of vegetation and surface temperature.
2. Another tool for comprehending topographic variations and evaluating geohazard susceptibility through its high-resolution elevation data is the Global Digital Elevation Model (GDEM). It can be seamlessly integrated with other geospatial datasets, including satellite imagery and geological information. This integration enhances the

understanding of how elevation influences the occurrence and impact of geohazards and provides a comprehensive view of the landscape. The elevation information derived from GDEM is essential for identifying and analyzing environmental factors that contribute to geohazard susceptibility and impact.

An analysis of GDEM data entailing calculations of slope, aspect, slope curvature, and Topographic Wetness Index (TWI) in order to identify the intricate topographic features was undertaken. Slope analysis provided understandings into the steepness of the terrain, while aspect revealed the directional orientation of the slopes. Slope curvature provided valuable information on the curvature characteristics of the landscape. Furthermore, the Topographic Wetness Index, where higher pixel values indicate an increased likelihood of the presence of water, contributed significantly to our understanding of hydrological aspects. These refined terrain descriptors provide insight into deciphering the intricate topographic nuances of the study region. This comprehensive analytical approach significantly enriches our understanding of the complexity of the landscape and makes a substantial contribution to the scientific discourse on environmental studies [24].

3. Lithological data are typically represented as a vector layer in GIS formats. This vector layer contains information on the geological composition of the area of study, including rock types, their distribution, and geological formations. For instance, areas characterized by loose or unconsolidated sediments may be more susceptible to landslides, whereas areas comprising certain types of rock may exhibit greater resistance to erosion. The integration with satellite and imagery data enables researchers to analyze the manner in which geological characteristics interact with topography and land cover to influence the occurrence of geohazards [13,19,30,39].
4. Tectonic structure data are typically represented as a vector layer in GIS formats, highlighting in particular the location and characteristics of fault lines. This vector layer provides crucial information on the presence, orientation, and activity of faults. High-resolution fault data are essential for seismic hazard assessment and for understanding the specific faults that may contribute to earthquakes and associated ground motions [16,26].
5. Land use data are typically represented as a vector layer in GIS formats and categorizes the manner in which land is utilized, including residential, commercial, agricultural, and industrial purposes. These data offer insights into the spatial distribution of human activities. An understanding of land use patterns is essential for the assessment of the contribution of human activities to or mitigation of geohazards. The processes of urbanization, deforestation, agriculture, and infrastructure development can all influence the vulnerability of an area to hazards such as landslides, erosion, and subsidence.
6. Rainfall directly affects hydrological processes, contributing to surface runoff, soil erosion, and slope saturation. Intense or prolonged rainfall events can trigger landslides, flash floods, and other geohazards, particularly in areas with steep terrain. Integrating rainfall data with other environmental datasets, such as topography, soil types, and land use, provides a holistic understanding of how precipitation interacts with the landscape [23,29,32].
7. Rivers play a key role in hydrological processes, influencing water distribution, sediment transport, and soil erosion by transporting sediment downstream. River data help to assess the potential for bank erosion and sediment deposition, which can affect the stability of adjacent slopes and contribute to geohazards.
8. Groundwater affects the stability of subsurface materials and geological formations. Groundwater exerts a profound influence on the stability of subsurface materials and geological formations. A change in the level of groundwater can result in land subsidence, which can in turn affect the stability of infrastructure and landscapes [34].
9. The road network can both contribute to and be impacted by geohazards. The occurrence of slope instability, landslides, and other hazards maximizes a reduction in

the stability of roads, thereby leading to disruptions and potential safety risks. It is therefore important to understand the spatial distribution of roads in order to assess their vulnerability to geohazards.

10. The peak ground acceleration (PGA) is a fundamental parameter for the comprehension of the potential impact of seismic events on structures and landscapes. PGA data indicate the level of ground shaking and are instrumental in assessing the vulnerability of buildings, infrastructure, and natural features to earthquake-induced geohazards. PGA values play a significant role in the development of building codes and seismic design standards. An understanding of the spatial distribution of peak ground acceleration (PGA) enables the implementation of construction practices that can withstand seismic forces, thereby reducing the risk of structural damage during earthquakes. It is reassuring to note that the peak ground acceleration (PGA) in the PHP area is relatively low at 0.16 g −s [16]. A low PGA value indicates a reduced probability of strong ground shaking during seismic events. The lower bound earthquake magnitude represents the threshold below which non-damaging earthquakes are excluded from the hazard analysis. In this study, the threshold is set at a magnitude of 5 for all source zones, as earthquakes below this magnitude are not potentially damaging for well-engineered structures [26,27,57,61].

3.2.2. Data for Information Procedures—Geospatial Analysis

The following advanced geospatial information calculations on the primary data were employed in order to create the appropriate GIS layers:

a. Satellite image processing (zoned vegetation density map (NDVI), zoned land surface temperature (LST) map, zoned map of the Topographical Wetness Index (TWI)).
b. Digital terrain model processing (zoned topography slope map, zoned relief aspect map, zoned map of slope curvature).
c. Lithology processing (zoned lithology map for each geohazard).
d. Faults processing (zoned fault map).
e. Land use processing (zoned land use map).
f. Rainfall—Daily calculations (zoned rainfall map).
g. Surface water processing (zoned river network map, distances from the hydrographic network).
h. Groundwater processing (zoned groundwater map).
i. Calculation of zoned road distance map
j. Zoned PGA map.

The layers of factors involved in geohazard GH1 are introduced below. Similarly, factor layers are calculated for the other five geohazards.

1. Satellite imagery was used to identify environmental indicators while processing data on factors influencing geohazards in the PHP area. The calculation of a vegetation density map involved classifying satellite data to represent different levels of vegetation cover, which was then normalized for standardized assessment. The resulting NDVI raster layer in the GIS platform provided a spatial overview of vegetation health (Figure 11a).
   Layer legend: NDVI indicates whether the target being observed contains live green vegetation or not (resulting values range from −1 to +1). Values close to +1 indicate high vegetation density and health. Values near 0 suggest barren areas of rock, sand, or snow. Negative values indicate water, snow, or clouds.
   The legend represents in color standardized ratings 0–100 for NDVI classes: 0.7–0.53, 0.53–0.36, 0.36–0.19, 0.19–0.02, 0.02−0.15, 0.
   A surface temperature map was also produced using similar classification and normalization procedures, resulting in a Land Surface Temperature (LST) raster GIS layer that captured temperature variations (Figure 11b).
   Layer legend: The LST index represents the temperature of the earth's surface as measured from satellite or ground-based observations. The legend represents in

color standardized ratings 0–100 for LST classes: 24–27.80, 27.80–31.60, 31.60–35.40, 35.40–39.20, 39.20–43.

A Topographic Wetness Index (TWI) map was produced by classifying and normalizing topographic wetness to facilitate understanding of the distribution of moisture across the landscape (Figure 11c).

Layer legend: The TWI is a numerical index that represents the spatial distribution of soil moisture in a landscape, based on its topography. The legend represents in color standardized ratings 0–100 for TWI classes: 22.5–18.38, 18.38–14.26, 14.26–10.14, 10.14–6.02, 6.02–1.9, <1.8.

The processed layers serve as critical inputs for geohazard vulnerability assessment, providing understanding of vegetation health, surface temperature patterns, and topographic wetness characteristics within the study region. The integration of remote sensing techniques enhances the accuracy of environmental assessments and contributes to a comprehensive understanding of the factors influencing geohazard vulnerability.

2. The Digital Elevation Model (DEM) was processed to derive topographic features to improve the understanding of terrain characteristics that influence geohazards in the PHP area. To produce a slope map, the DEM was classified to delineate different Slope classes, which were then normalized for standardized presentation. The resulting raster layer provided insight into the variations in terrain steepness (Figure 12a).

   Layer legend: The legend represents in color standardized ratings 0–100 for Slope classes, Escarpments, >35, Steep slopes, 25–35, Moderately steep slopes, 15–25, Genie slopes, 5–15, Very gentle slopes, <5.

   At the same time, an aspect map was produced, resulting in a raster layer showing terrain orientations. This information helps to identify landscape features that are influenced by slope direction (Figure 12b).

   Layer legend: The legend represents in color standardized ratings 0–100 for Aspect classes: >270, 180–270, 90–180, <90.

   A curvature map was also produced. The resulting raster layer provides understanding of variations in terrain shape, which helps in the assessment of geological vulnerability associated with curvature characteristics (Figure 12c).

   Layer legend: The legend represents in color standardized ratings 0–100 for Curvature classes: <-1.5, -1.5–-0.5, -0.5–0, >0.

   These processed maps serve as an essential input to geohazard assessments, providing a comprehensive perspective on the topographic nuances that influence the vulnerability of the region under study to various hazards.

3. Regarding lithology, a careful grouping and ranking of geological formations, assigning values corresponding to each specific geohazard category, is performed. The vector layers representing the lithological formations were then converted into raster layers and normalized to ensure a consistent representation across the area of study (Figure 13). The resulting zoned lithology raster layers provide insight into the spatial distribution and characteristics of geological formations that influence various geohazards.

   Layer legend: Assigned values from 0 to 100 to different types of bedrock (lithology map). Lower values indicate a lower risk of landslides, while higher values indicate a higher risk of landslides. Flysch 100, Scree 87.5, Alluvial, Ophiolites 75, Keratolites, Conglomerate rock 62.5, Marls, Clays, Sands 50, Lignite strata, Sandstones 37.5, Limestones, River terraces 25.

4. Focusing on faults, a zoned fault map was produced using a multi-step approach. First, a raster layer was created showing the distance to each fault, which facilitated the assessment of proximity to fault lines. This raster layer was then subjected to classing, normalization, and the construction of a zoned fault map (Figure 14).

   Layer legend: The legend represents in color standardized ratings 0–100 for Faults classes: <150 m, 150–300 m, >300 m.

The layer delineates the proximity of faults and provides important insight into the spatial distribution of faults and their potential impact on geohazard susceptibility.

5. Regarding the land use, a zoned map was meticulously calculated. A comprehensive classification and ranking of land use categories on a scale based on their susceptibility to settlement was carried out. Normalization was then applied to standardize the land use values, and the subsequent transformation of four vector layers into raster layers facilitated consistent analysis (Figure 15).
Layer legend: The legend represents in color standardized ratings 0–100 for Land Use 10 classes, Mineral Extraction sites: 100, Burnt areas: 90—Industrial and Commercial Units, Non-irrigated Arable: 80, Land Road and Rail Networks: 70, Discontinuous Urban Fabric: 60, Transitional Woodland Shrubs: 50, Water bodies: 40, Complex Cultivation Patterns—Principally agriculture with Natural Vegetation, Beaches—Dunes and Sand Plains: 30, Olive Groves—Pastures—Mixed Forest: 20, Broad-leaved Forest—Coniferous Forest—Natural Grassland, Moors, and Heathland—Sclerophyllous Vegetation: 10.
The resulting zoned land use map provides a structured representation of land use categories, providing insight into the spatial distribution of land cover and its correlation with geohazard susceptibility.
6. As part of the rainfall processing, a zoned rainfall map was created to understand the spatial distribution of precipitation patterns. The process involved the creation of classes categorizing levels of rainfall intensity. Normalization was then applied to ensure consistent representation of rainfall values. The culmination of these steps resulted in the development of a raster layer illustrating zoned rainfall, providing critical understanding to variations in rainfall intensity (Figure 16). This zoned rainfall map is essential for understanding the localized impact of rainfall on geohazards such as landslides and erosion, enabling effective risk assessment and management strategies. Classes 0–1, 1–2, 2–3, 3–4, 4–5 (rainfall).
7. For the surface water data, with a particular focus on rivers, a zoned river map was computed to assess the proximity of rivers. The process began with the conversion and construction of a raster layer mapping the distance to each river. The zoned river map serves as a valuable resource for understanding the relationship between surface water characteristics and geological vulnerability, assisting in the identification of areas prone to river-related geohazards and contributing to targeted risk mitigation strategies.
With regard to groundwater, a zonal map was also produced to delineate the distribution of underground water sources. The procedure involved the establishment of classes based on groundwater levels, followed by a normalization process to ensure a consistent representation. A raster layer was then generated that provides understanding of the spatial distribution of groundwater resources and highlights their potential impact on landscape dynamics. The zoned groundwater map is proving to be a valuable tool for understanding the complex interplay between groundwater dynamics and the evolving characteristics of the terrain. It helps to identify areas susceptible to groundwater-influenced change and provides a basis for tailored strategies to understand and manage these landscape dynamics.
A developed zoned map provided a detailed overview of the spatial proximity of road networks across the PHP area. The process began with the conversion and construction of a raster layer that recorded the distance from each road. The raster layer was then categorized and normalized, culminating in the creation of a zoned road network map. The layer provides an understanding of the influence of road networks on the surrounding terrain. The zoned road network map is proving to be a key tool for unraveling the impacts of transport networks, helping to identify regions shaped by road infrastructure, and contributing to land-use planning strategies.
As part of the PGA processing, the analysis produced a zoned map detailing the maximum ground acceleration across the PHP. A raster layer was generated showing

the zoned map of maximum ground acceleration with the values standardized accordingly. This map provides understanding of the varied spatial distribution of ground acceleration, thus providing a detailed perspective on seismic characteristics as required by GreDaSS [62]. The zoned PGA map is a valuable tool for understanding the diverse seismic conditions within the area of study, providing valuable information for strategic decision-making in infrastructure development and seismic risk mitigation.

In the following figures, the park boundary is represented by the yellow polygonal line.

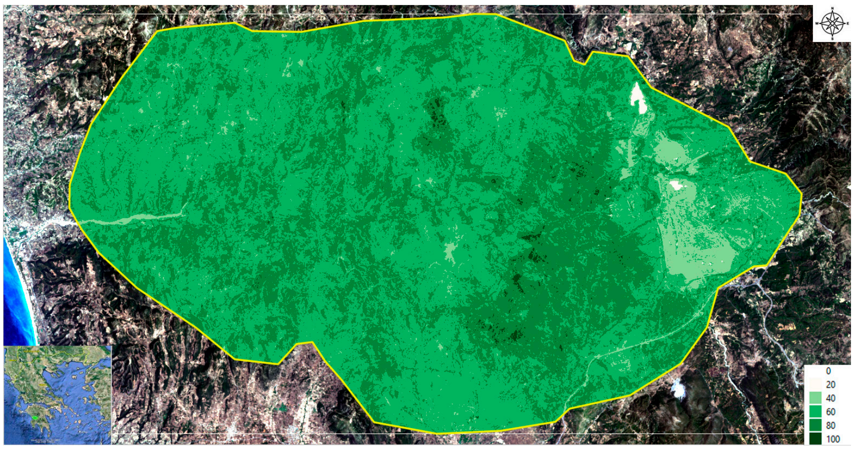

(**a**)

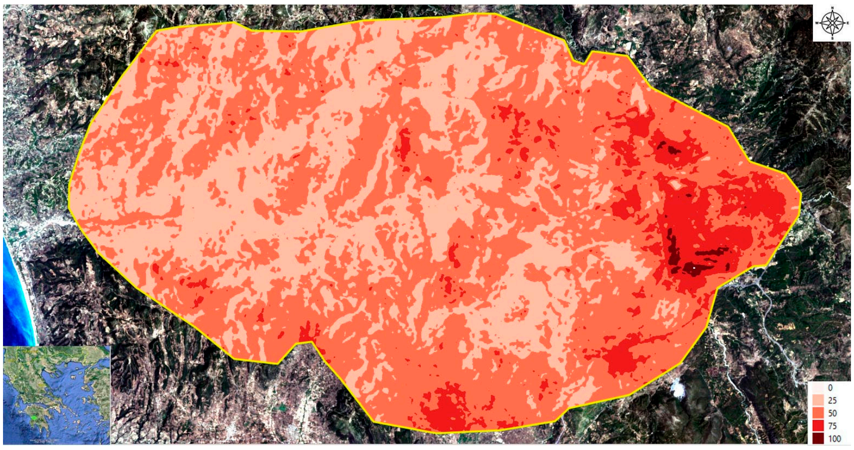

(**b**)

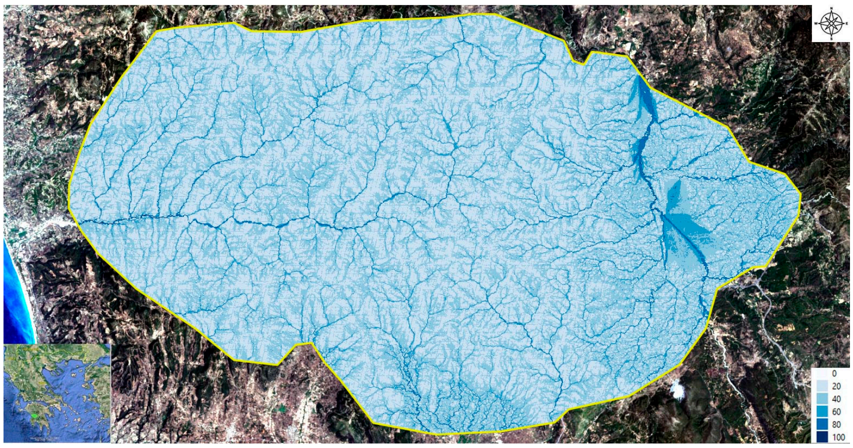

(**c**)

Figure 11. (**a**) NDVI raster layer. (**b**) Land Surface Temperature (LST) raster layer. (**c**) Topographic Wetness Index (TWI) raster layer.

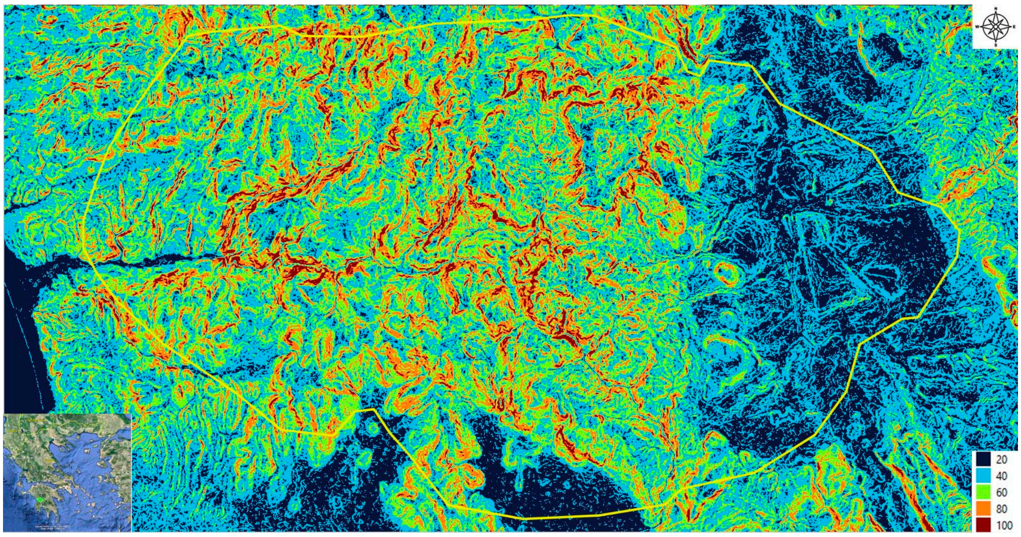

(**a**)

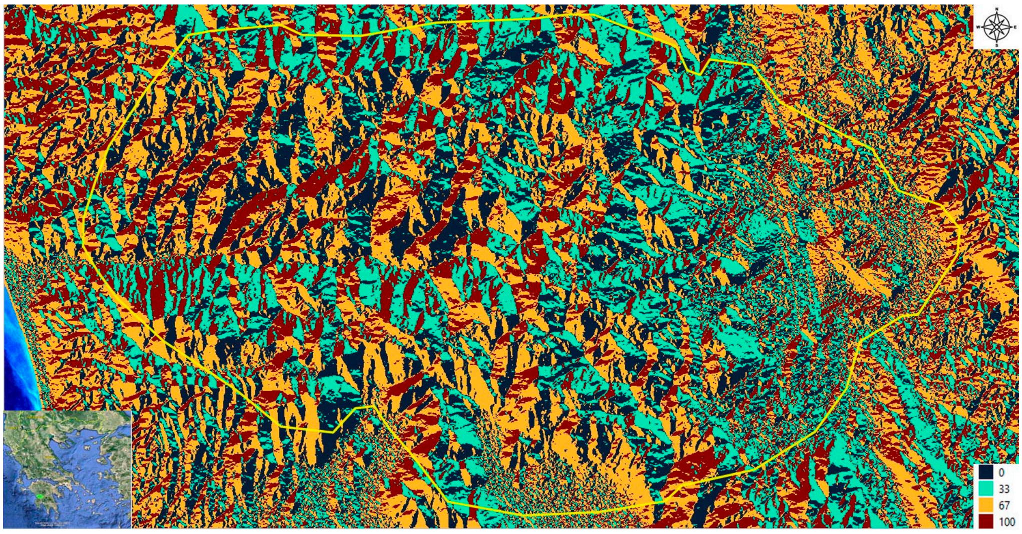

(**b**)

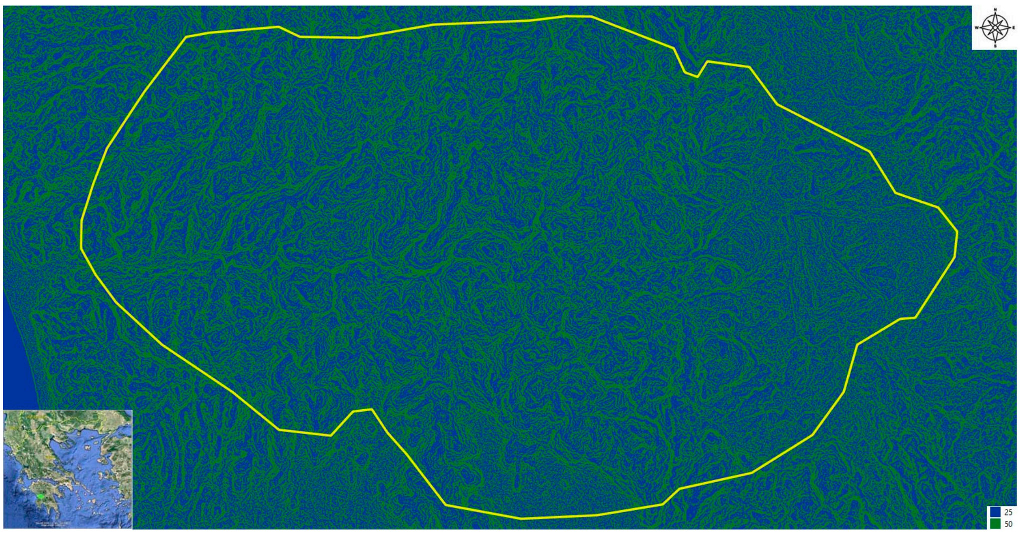

(**c**)

Figure 12. (**a**) Slope raster layer. (**b**) Aspect raster layer. (**c**) Curvature raster layer.

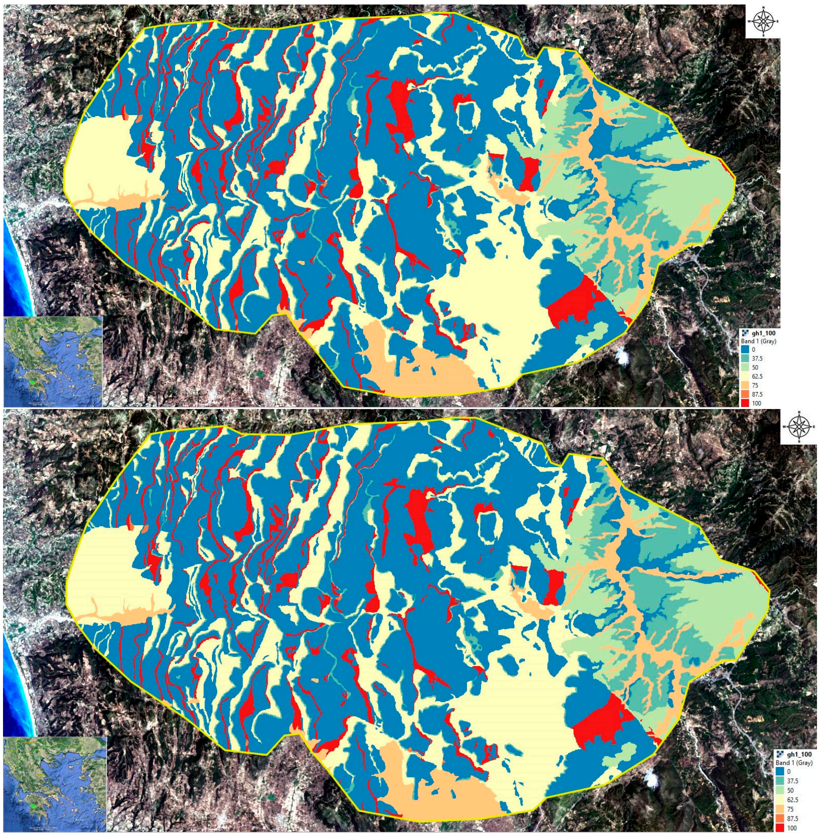

Figure 13. Lithology raster layer.

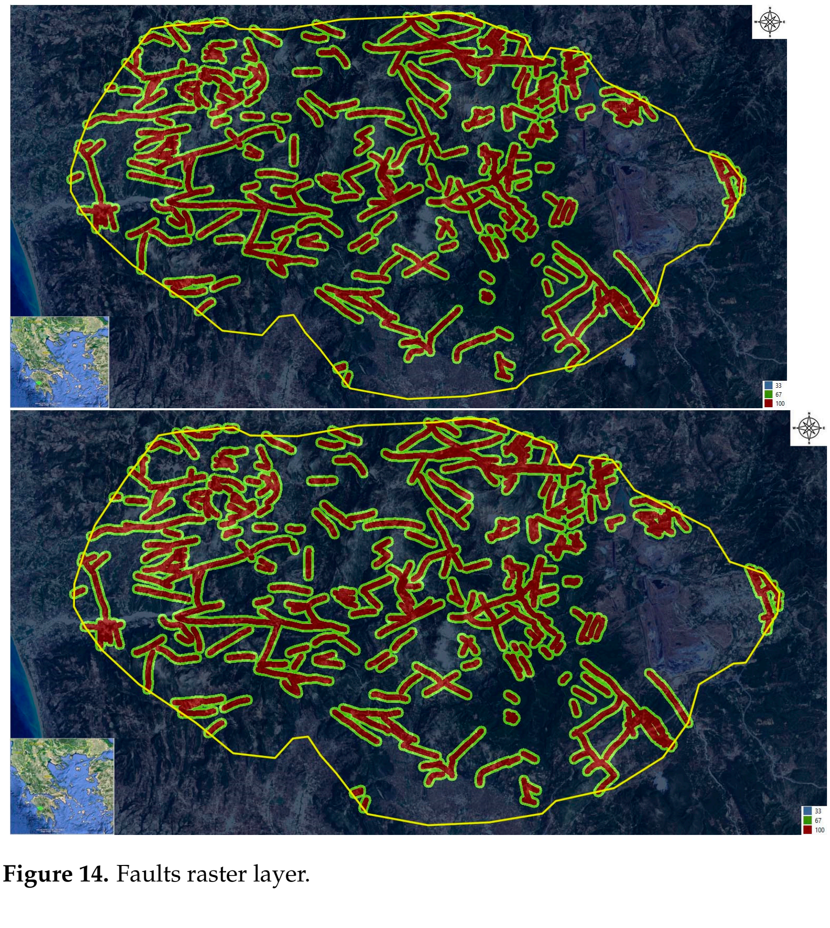

Figure 14. Faults raster layer.

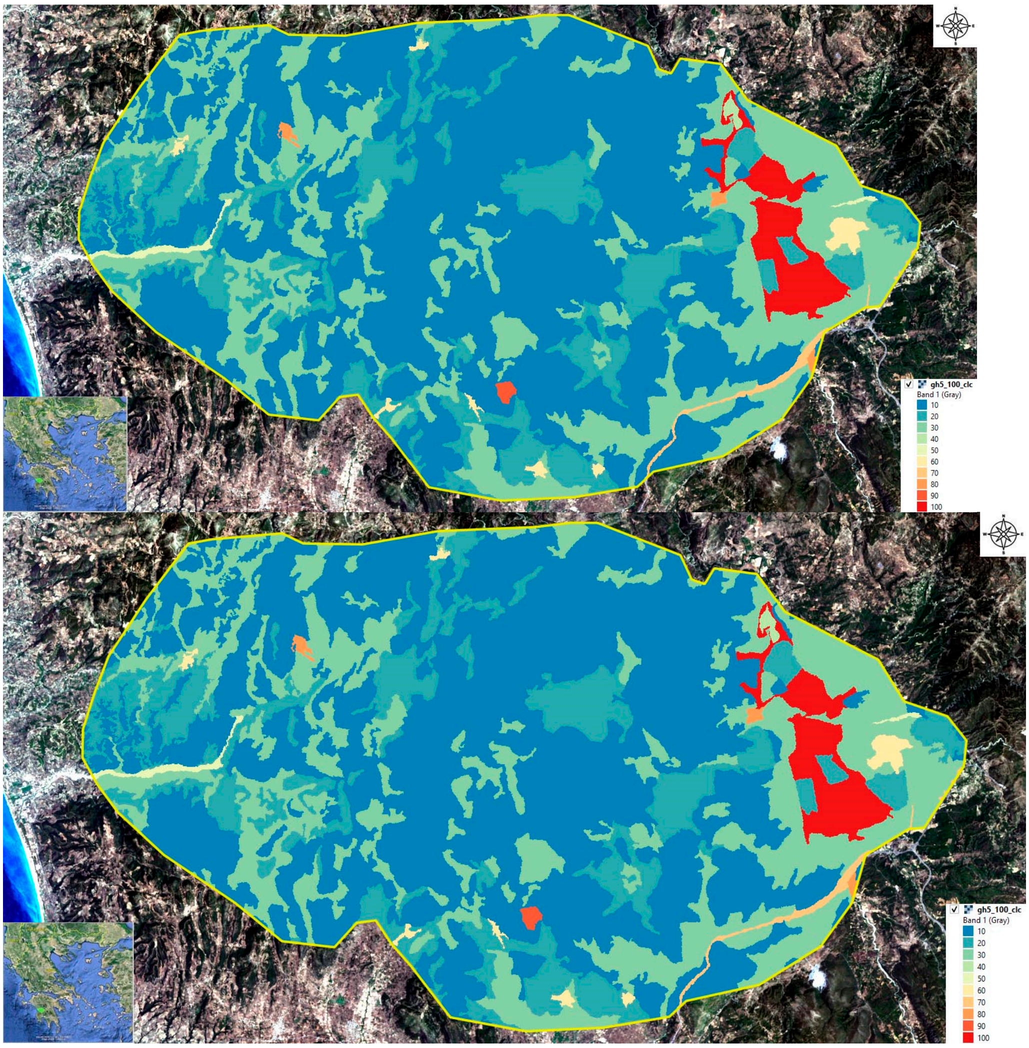

Figure 15. Land-use raster layer.

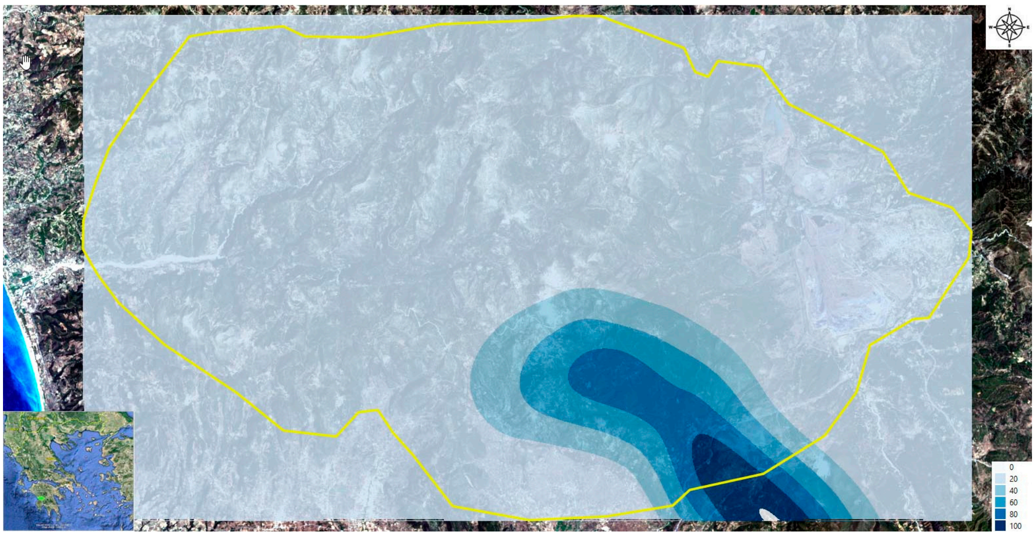

Figure 16. Rainfall (summer data) raster layer.

3.3. Geohazards Prevention Index (GPI) Implementation

The GPI is initiated at two distinct phases. At the initial phase, geohazard maps are calculated on a geohazard-by-geohazard basis. Each geohazard, as described in the framework's functions C, D, and E, is the sum of the environmental factors contributing to each geohazard multiplied by the weight of their contribution to it. The weights are calculated using the AHP method. The calculated raster layers of each geohazard are then stored on the GIS platform. In the second and final phase, the cumulative geohazard is calculated as the sum of the previously calculated hazards for each geohazard, multiplied by the weight of each hazard's participation. The weights are substituted once more by applying the AHP method.

3.3.1. Generation of Zoned Hazard Map per Geohazard

Analytic Hierarchy Process (AHP) is an advanced scoring method that can be used to determine the relative importance and influence of each factor, in our case in the context of each geohazard. The method uses a series of pairwise comparisons to assess the importance of factors and determine their weights. It systematically assesses the relative importance of factors by considering all possible pairs and determining their importance in a consistent manner. By comparing factors based on a set of criteria, AHP allows the generation of weighted values that reflect the hierarchy and relative influence of each factor within the overall analysis.

The importance of each pairwise comparison in the method, in the case of PHP, was determined based on both an extensive review of the relevant literature and consultation with recognized experts in the field (interviewing geologists from the Kapodistrian University of Athens, the University of West Attica, and the University of Patras). With this knowledge, the comparison criteria were carefully evaluated to ensure a robust and informed assessment of the relative importance of the factors [12,40].

The calculations of the AHP method were performed using the original software of Spicelogic Inc., version 4.2.6.

(a) Below are the results of the method, presented with three figures for each geohazard. The first one in each set shows the Pairwise Comparison Matrix of the AHP. This matrix is of crucial importance, as it converts subjective assessments into a mathematical form, thereby enabling a systematic and objective decision-making process. It ensures that all criteria and alternatives are considered relative to one another and provides a method for verifying the consistency of these comparisons, thereby leading to more reliable and justifiable decisions.
The consistency ratio (CR) displayed in each figure is calculated to ensure that the comparisons are sufficiently consistent. A CR of less than 0.1 is generally considered acceptable. High inconsistency indicates the need for re-evaluation of the comparisons [40].
The calculations for the geohazards (GH), landslide (Figure 17), weathering (Figure 18), erosion (Figure 19), and subsidence (Figure 20) show very good CR values, so there is no need to recalculate the pairs.

(b) The second figure of the triad shows the relative priority of each factor involved in the formation of the geohazard in percentages.

(c) Finally, the third figure shows the calculated weights.

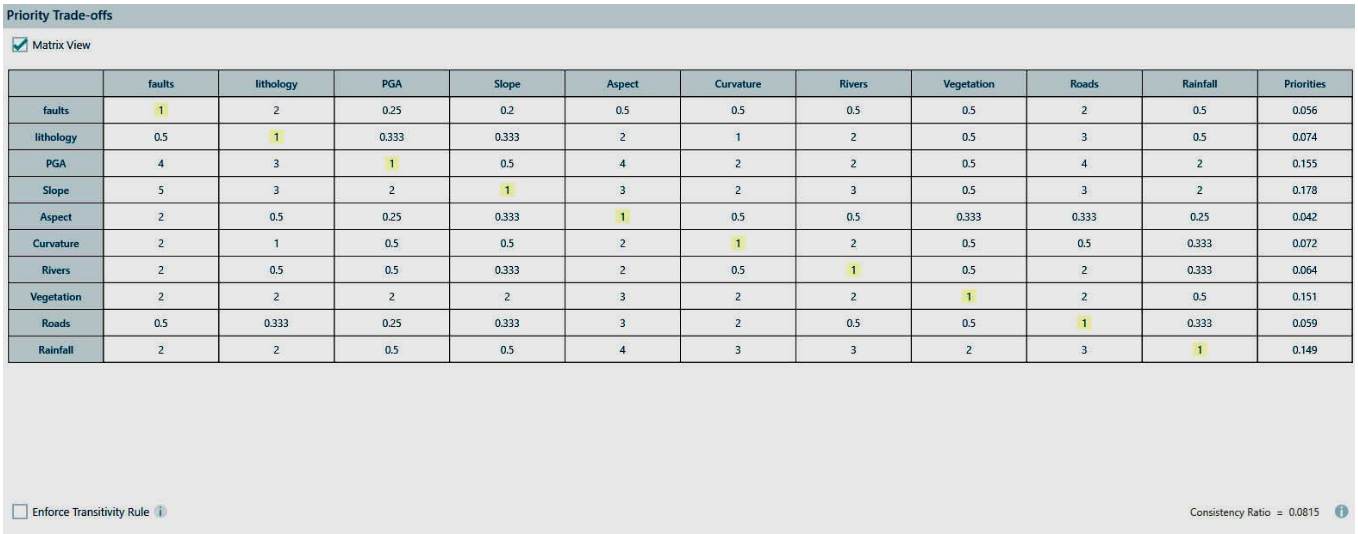

	faults	lithology	PGA	Slope	Aspect	Curvature	Rivers	Vegetation	Roads	Rainfall	Priorities
faults	1	2	0.25	0.2	0.5	0.5	0.5	0.5	2	0.5	0.056
lithology	0.5	1	0.333	0.333	2	1	2	0.5	3	0.5	0.074
PGA	4	3	1	0.5	4	2	2	0.5	4	2	0.155
Slope	5	3	2	1	3	2	3	0.5	3	2	0.178
Aspect	2	0.5	0.25	0.333	1	0.5	0.5	0.333	0.333	0.25	0.042
Curvature	2	1	0.5	0.5	2	1	2	0.5	0.5	0.333	0.072
Rivers	2	0.5	0.5	0.333	2	0.5	1	0.5	2	0.333	0.064
Vegetation	2	2	2	2	3	2	2	1	2	0.5	0.151
Roads	0.5	0.333	0.25	0.333	3	2	0.5	0.5	1	0.333	0.059
Rainfall	2	2	0.5	0.5	4	3	3	2	3	1	0.149

(**a**)

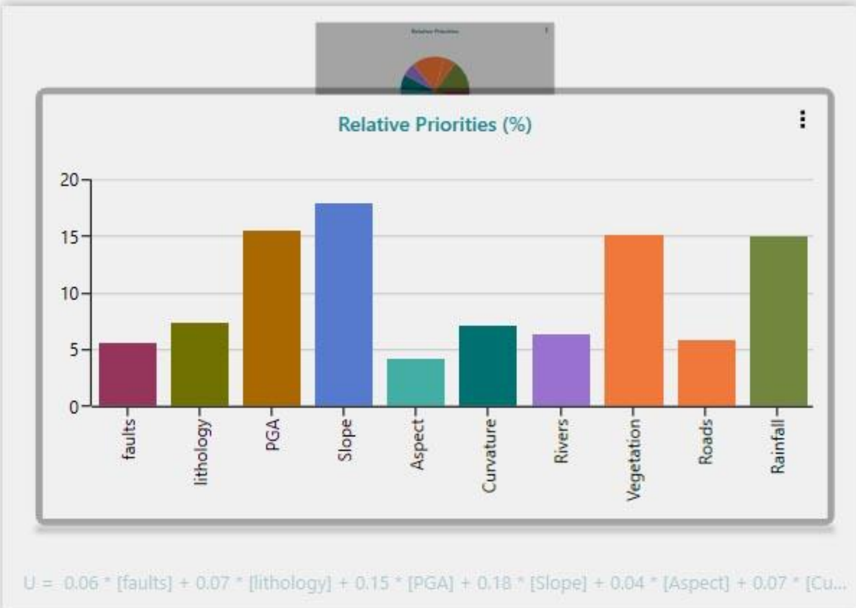

(**b**)

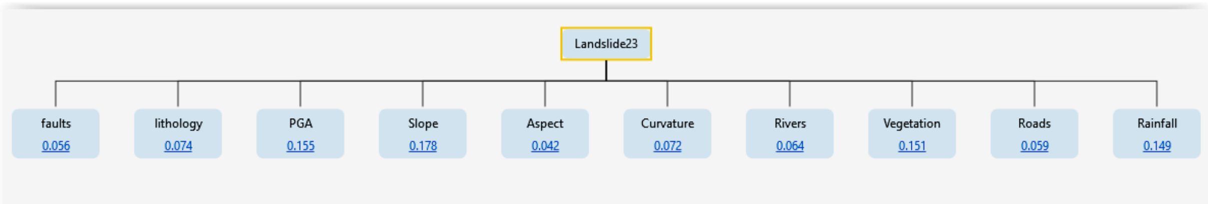

(**c**)

Figure 17. (**a**) Landslide Geohazard Pairwise AHP matrix. (**b**) Landslide AHP Relative Priorities diagram. Landslide: 0.06 × [faults] + 0.07 × [lithology] + 0.15 × [PGA] + 0.18 × [Slope] + 0.04 × [Aspect] + 0.07 × [Curvature] + 0.06 × [Rivers] + 0.15 × [Vegetation] + 0.06 × [Roads] + 0.15 × [Rainfall]. (**c**) Landslide AHP weight calculations: Faults 0.056, Lithology 0.074, PGA 0.155, Slope 0.178, Aspect 0.042, Curvature 0.072, Rivers 0.064, Vegetation 0.151, Roads 0.059, and Rainfall 0.149.

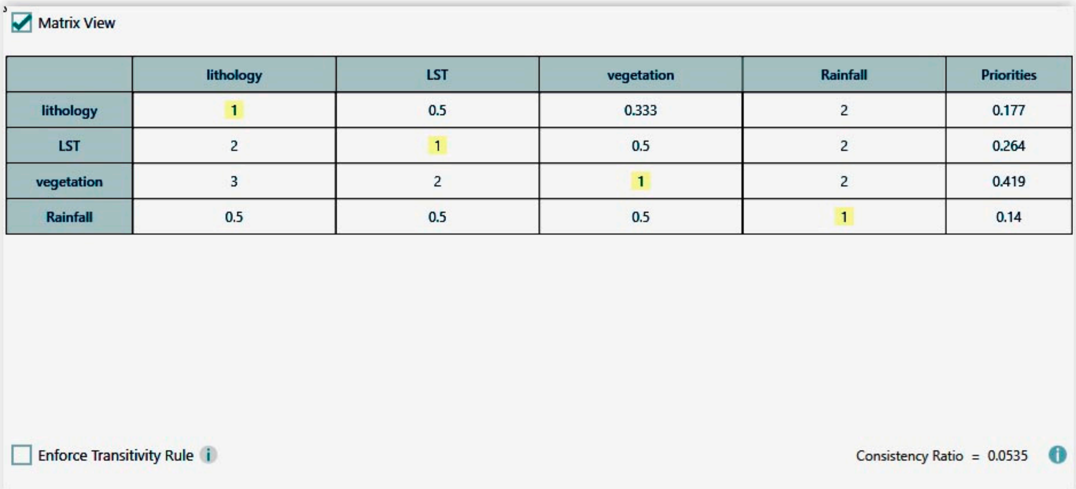

Matrix View

	lithology	LST	vegetation	Rainfall	Priorities
lithology	1	0.5	0.333	2	0.177
LST	2	1	0.5	2	0.264
vegetation	3	2	1	2	0.419
Rainfall	0.5	0.5	0.5	1	0.14

Enforce Transitivity Rule

Consistency Ratio = 0.0535

(**a**)

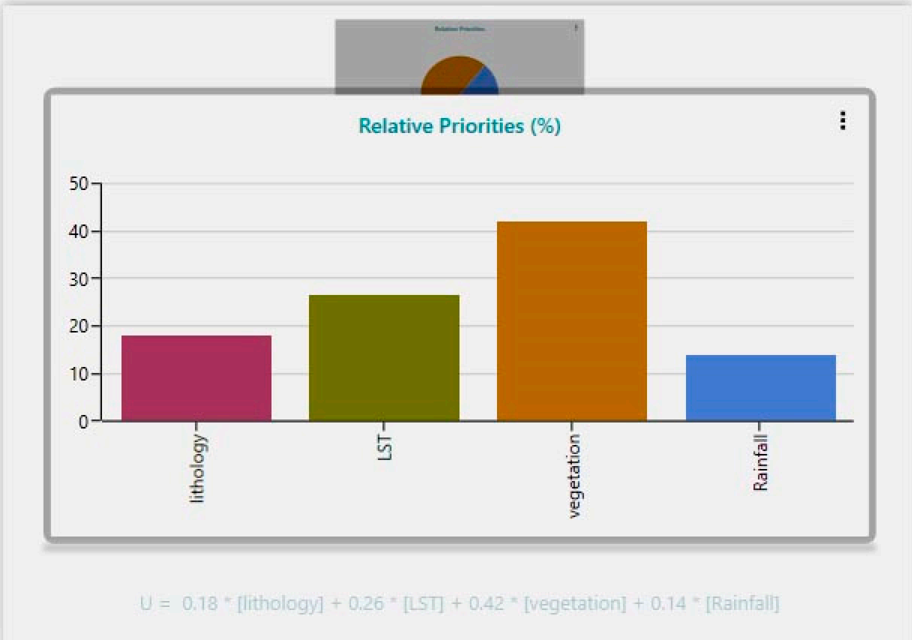

(**b**)

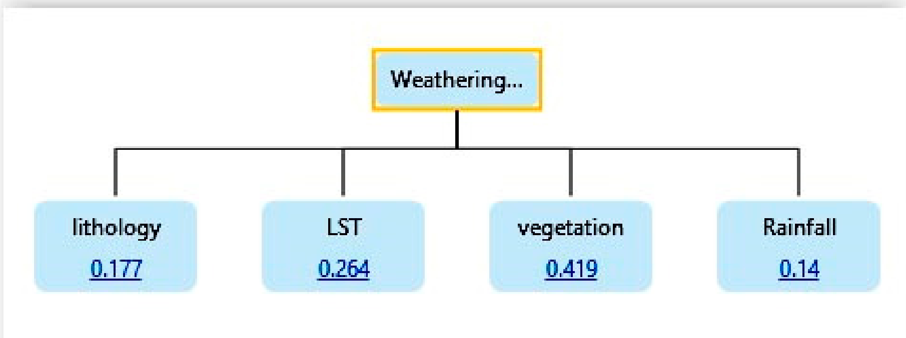

(**c**)

Figure 18. (**a**) Weathering Geohazard Pairwise AHP matrix. (**b**) Weathering AHP Relative Priorities diagram. Weathering: 0.18 × [lithology] + 0.26 × [LST] + 0.42 × [vegetation] + 0.14 × [Rainfall]. (**c**) Weathering AHP weight calculations.

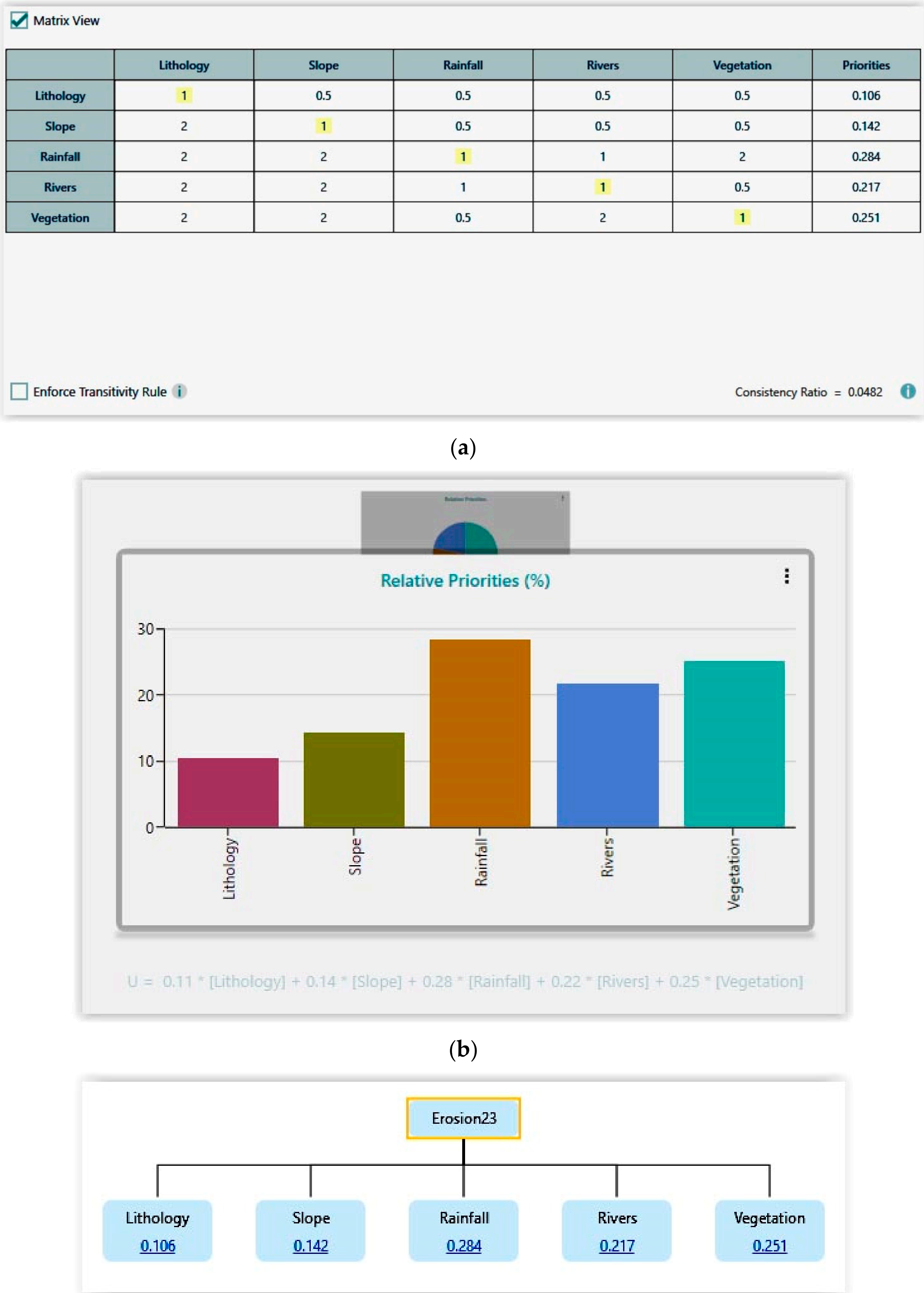

Matrix View

	Lithology	Slope	Rainfall	Rivers	Vegetation	Priorities
Lithology	1	0.5	0.5	0.5	0.5	0.106
Slope	2	1	0.5	0.5	0.5	0.142
Rainfall	2	2	1	1	2	0.284
Rivers	2	2	1	1	0.5	0.217
Vegetation	2	2	0.5	2	1	0.251

Enforce Transitivity Rule

Consistency Ratio = 0.0482

(**a**)

(**b**)

(**c**)

Figure 19. (**a**) Erosion Geohazard Pairwise AHP matrix. (**b**) Erosion AHP Relative Priorities diagram. Erosion: 0.11 × [Lithology] + 0.14 × [Slope] + 0.28 × [Rainfall] + 0.22 × [Rivers] + 0.25 × [Vegetation]. (**c**) Erosion AHP weight calculations.

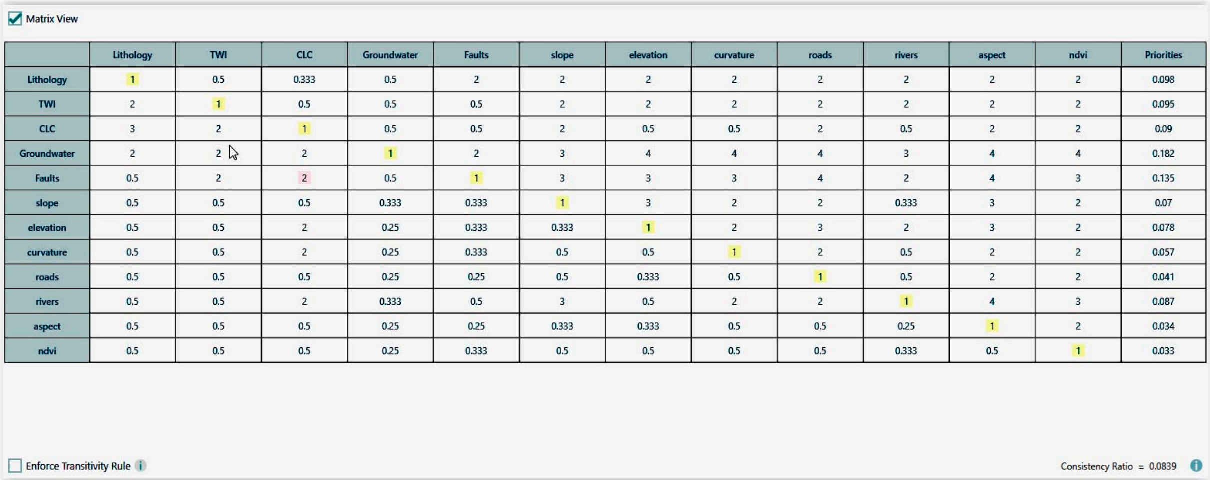

Matrix View

	Lithology	TWI	CLC	Groundwater	Faults	slope	elevation	curvature	roads	rivers	aspect	ndvi	Priorities
Lithology	1	0.5	0.333	0.5	2	2	2	2	2	2	2	2	0.098
TWI	2	1	0.5	0.5	0.5	2	2	2	2	2	2	2	0.095
CLC	3	2	1	0.5	0.5	2	0.5	0.5	2	0.5	2	2	0.09
Groundwater	2	2	2	1	2	3	4	4	4	3	4	4	0.182
Faults	0.5	2	2	0.5	1	3	3	3	4	2	4	3	0.135
slope	0.5	0.5	0.5	0.333	0.333	1	3	2	2	0.333	3	2	0.07
elevation	0.5	0.5	2	0.25	0.333	0.333	1	2	3	2	3	2	0.078
curvature	0.5	0.5	2	0.25	0.333	0.5	0.5	1	2	0.5	2	2	0.057
roads	0.5	0.5	0.5	0.25	0.25	0.5	0.333	0.5	1	0.5	2	2	0.041
rivers	0.5	0.5	2	0.333	0.5	3	0.5	2	2	1	4	3	0.087
aspect	0.5	0.5	0.5	0.25	0.25	0.333	0.333	0.5	0.5	0.25	1	2	0.034
ndvi	0.5	0.5	0.5	0.25	0.333	0.5	0.5	0.5	0.5	0.333	0.5	1	0.033

Enforce Transitivity Rule

Consistency Ratio = 0.0839

(**a**)

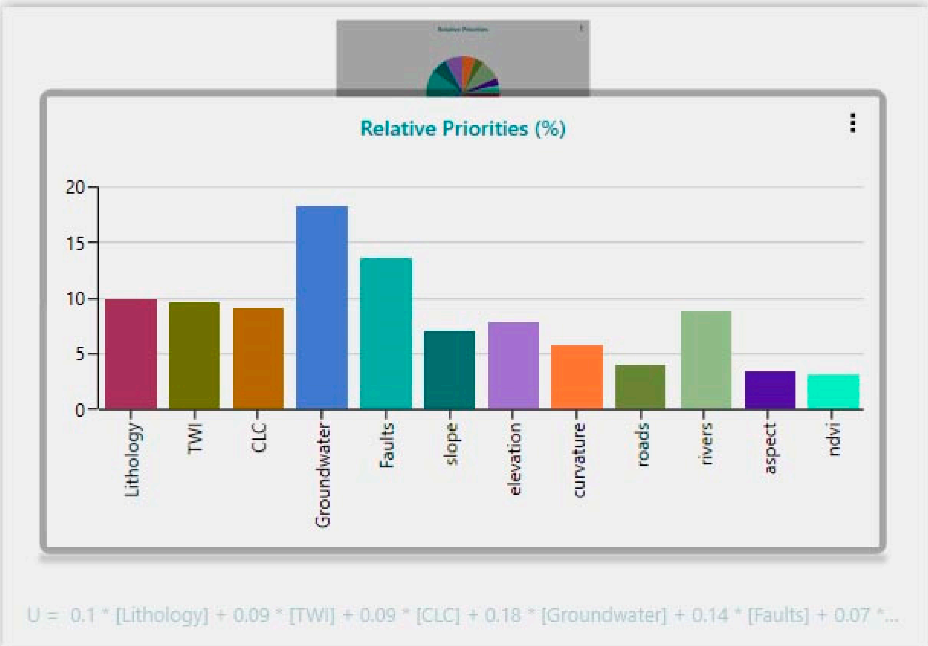

(**b**)

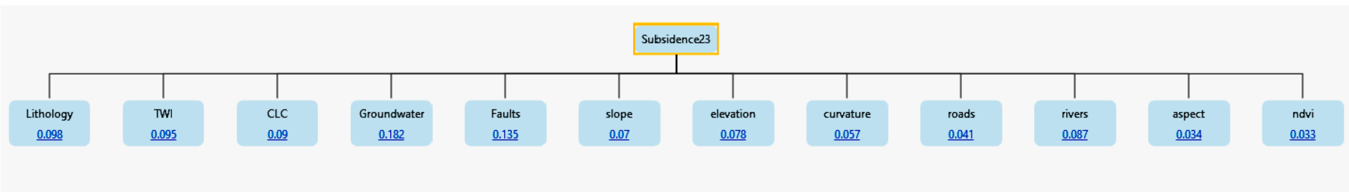

(**c**)

Figure 20. (**a**) Subsidence Geohazard Pairwise AHP matrix. (**b**) Subsidence AHP Relative Priorities diagram. Subsidence: 0.1 × [Lithology] + 0.09 × [TWI] + 0.09 × [CLC] + 0.18 × [Groundwater] + 0.14 × [Faults] + 0.07 × [slope] + 0.08 × [elevation] + 0.06 × [curvature] + 0.04 × [roads] + 0.09 × [rivers] + 0.03 × [aspect] + 0.03 × [ndvi]. (**c**) Subsidence AHP weight calculations: Lithology 0.098, TWI 0.095, CLC 0.09, Groundwater 0.182, Faults 0.135, Slope 0.07, Elevation 0.078, Curvature 0.057, Road Network 0.041, Rivers 0.087, and Aspect 0.034, NDVI 0.033.

3.3.2. Generation of Cumulative Geohazard Zoned Map

The weighted contribution of geohazards to the Geohazards Prevention Index (GPI) was once again calculated using the Analytic Hierarchy Process (AHP) method [40]. This involved an exhaustive pairwise comparison of the geohazards, taking into account their relative importance in the context of the GPI. As previously, the importance of each pairwise comparison in the method in the case of the PHP was determined again. The calculated CR is highly satisfactory (Figure 21). The AHP facilitated a systematic evaluation of the geohazards by assigning weights based on their hierarchical importance. The method provided a comprehensive understanding of the individual contributions of geohazards to the overall GPI.

Matrix View

	Landslide	Earthquake	Weathering	Erosion	Subsidence	Priorities
Landslide	1	6	4	3	1	0.365
Earthquake	0.167	1	0.333	0.333	0.2	0.051
Weathering	0.25	3	1	0.333	0.25	0.092
Erosion	0.333	3	3	1	2	0.235
Subsidence	1	5	4	0.5	1	0.257

Enforce Transitivity Rule

Consistency Ratio = 0.0830

(**a**)

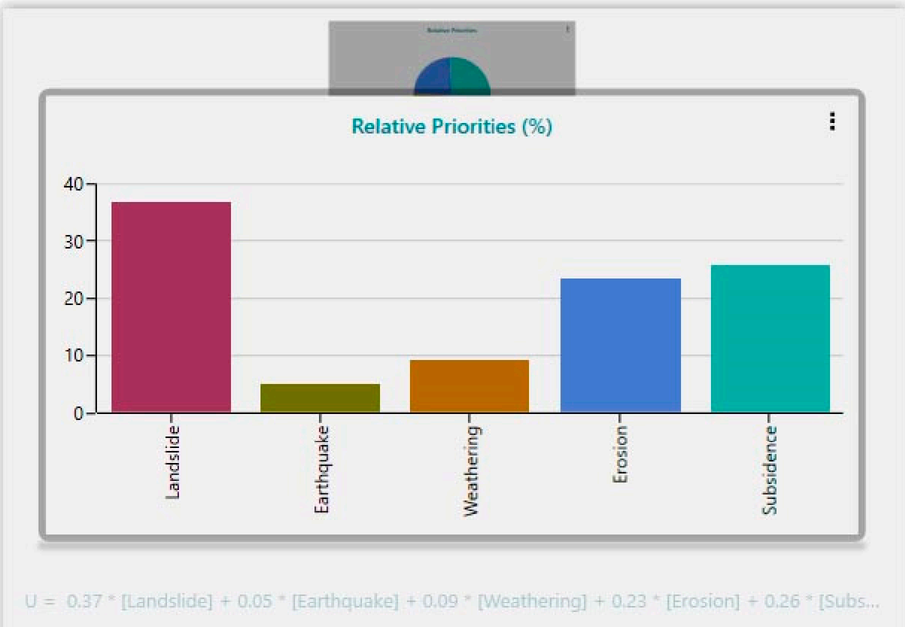

(**b**)

Figure 21. *Cont.*

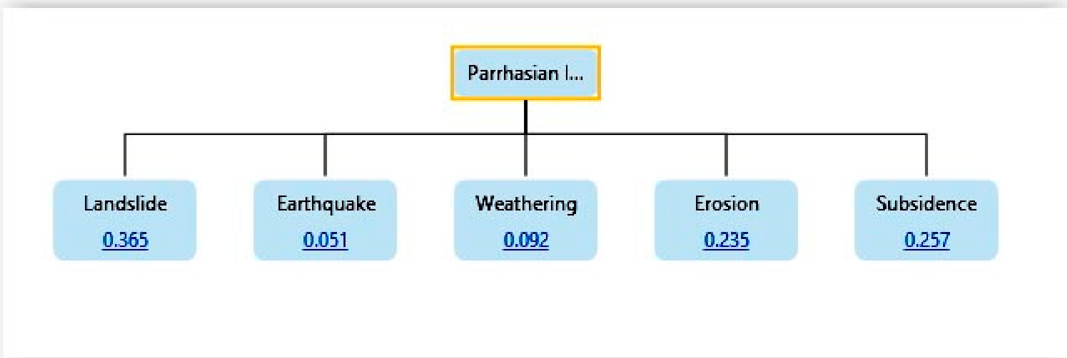

(**c**)

Figure 21. (**a**) Cumulative Geohazards Pairwise AHP matrix. (**b**) Cumulative Geohazards AHP Relative Priorities diagram. GPI: 0.37 × [Landslide] + 0.05 × [Earthquake] + 0.09 × [Weathering] + 0.23 × [Erosion] + 0.26 × [Subsidence]. (**c**) Cumulative Geohazards AHP weight calculations.

The Geohazards Prevention Index (GPI) was employed to generate the Cumulative Geohazard Assessment Map, presented in Figure 22, of the Parrhasian Heritage Park of the Peloponnese.

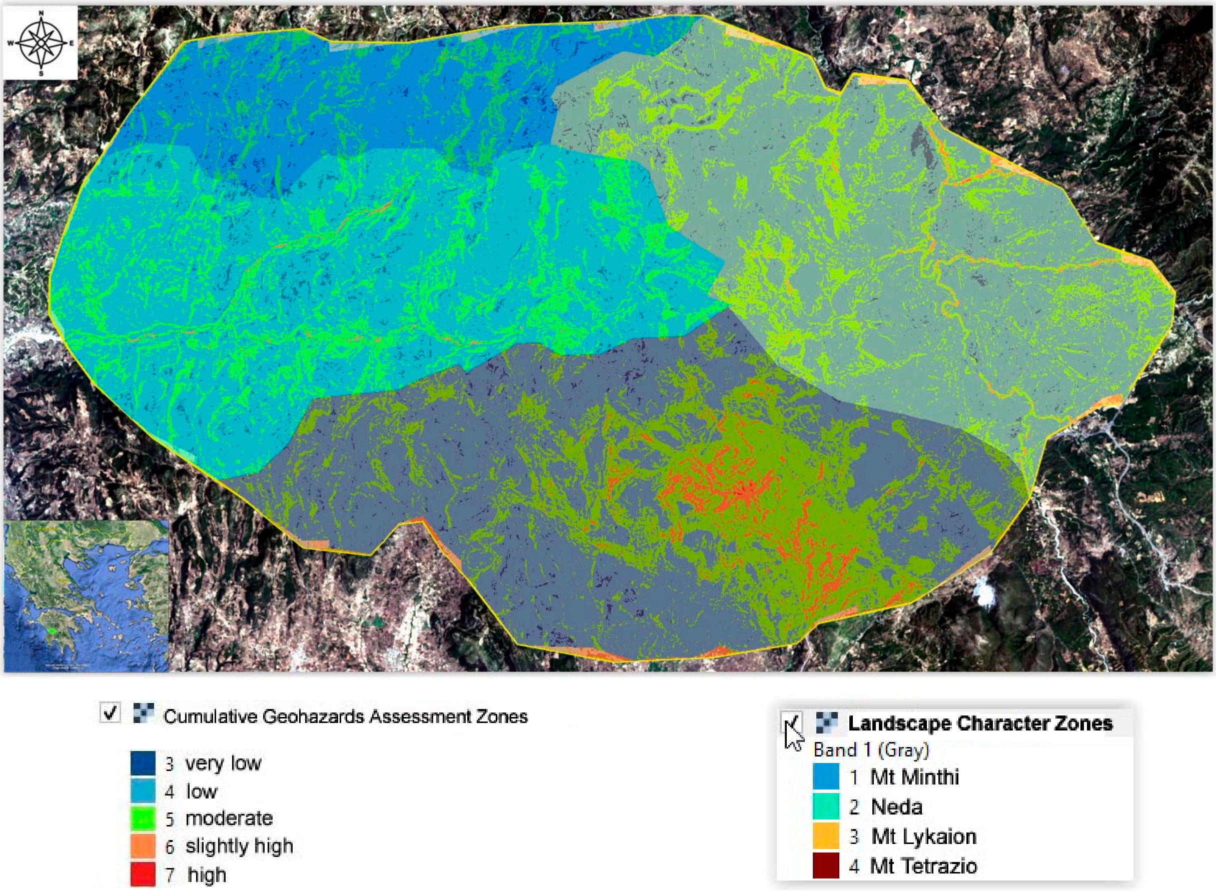

Figure 22. Parrhasian Heritage Park—Cumulative Geohazard Assessment Map.

Legend: 1—Insignificant; 2—Extremely Low; 3—Very Low; 4—Low; 5—Moderate; 6—Slightly High; 7—High; 8—Very High; 9—Extremely High; and 10—Critically High [42].

Figure 23 presents two three-dimensional views of the Cumulative Geohazard Assessment Map.

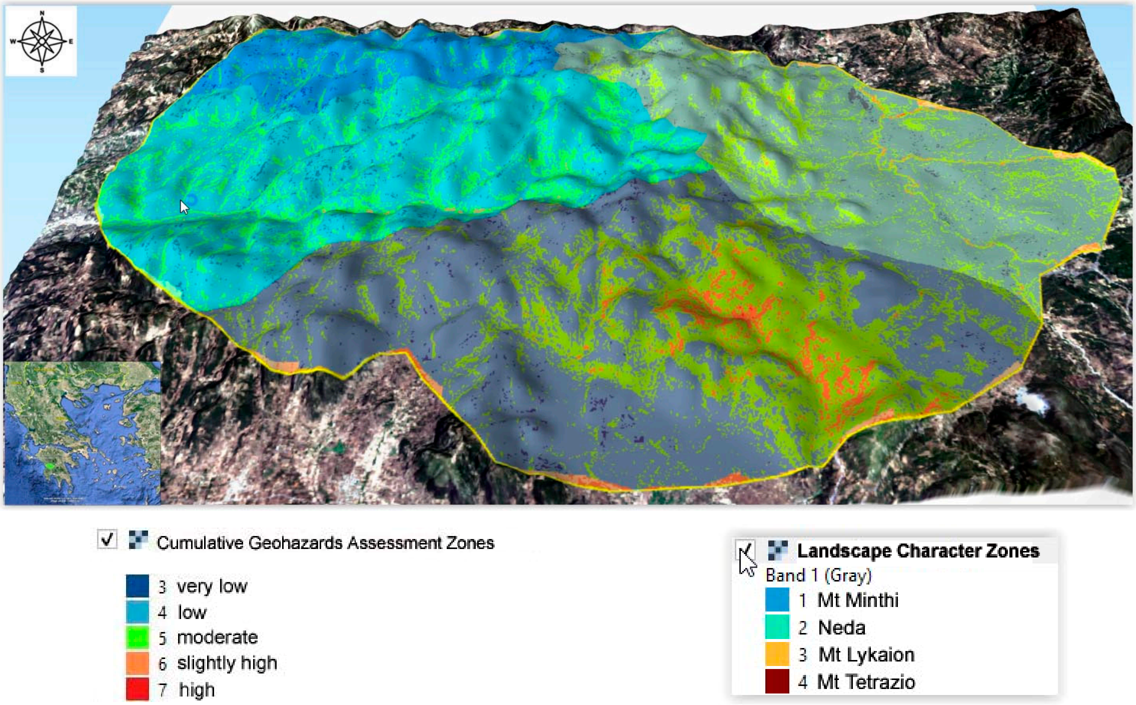

(**a**)

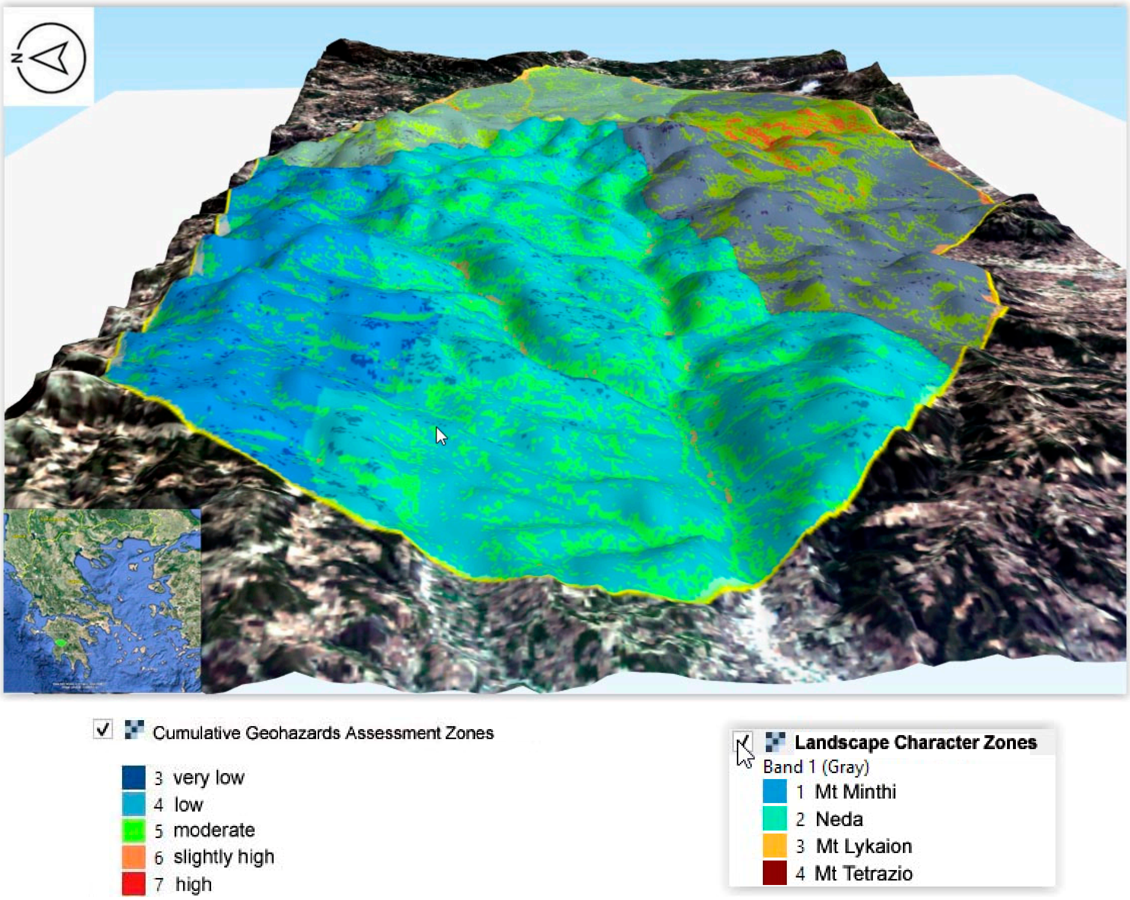

(**b**)

Figure 23. Parrhasian Heritage Park—Cumulative Geohazard Zoned Map. (**a**) Three-dimensional view from south Mt. Tetrazio landscape zone. (**b**) Three-dimensional view from west Neda and Mt. Minthi landscape zones.

In Figure 23a the distinctive relief of the four landscape character zones is depicted. The mountainous zone of Mt. Minti (zone 1) in the north and the mountainous zone of Mt. Tetrazion in the south (zone 4) collectively form an envelope that encloses the Mt. Lykaion Zone (zone 3) in the east and the Neda Zone (zone 2) in the west.

This envelope is characterized by an extraordinary gorge with the Neda River that leads to the west, at the Kyparissiakos Gulf.

Figure 23b is eastward oriented, and the full expanse of the Neda River gorge is visible. The characteristic mountainous envelope is also evident in the image.

3.3.3. Validation of Results (ROC Analysis)

The evaluation of the GPI was based on the Receiver Operating Characteristic (ROC) analysis. This is a powerful and widely used method for evaluating the performance of binary classification models. It is particularly useful for understanding the trade-offs between true positive rates (sensitivity) and false positive rates (specificity) at different threshold settings.

The visual output of the application is the ROC curve, a graphical plot that illustrates the diagnostic ability of the binary classifier system. It is generated by plotting the true positive rate against the false positive rate at various threshold settings. Each point on the ROC curve represents a sensitivity/specificity pair corresponding to a particular decision threshold [43].

In the graph (Figure 24), the x-axis represents the false positive rate, which is the percentage of true negatives that are incorrectly identified as positives by the model. The y-axis represents the true positive rate (sensitivity), which is the percentage of true positives correctly identified by the model. For specific geohazard points on the Cumulative Geohazard Zoned Map, the ground situation was observed.

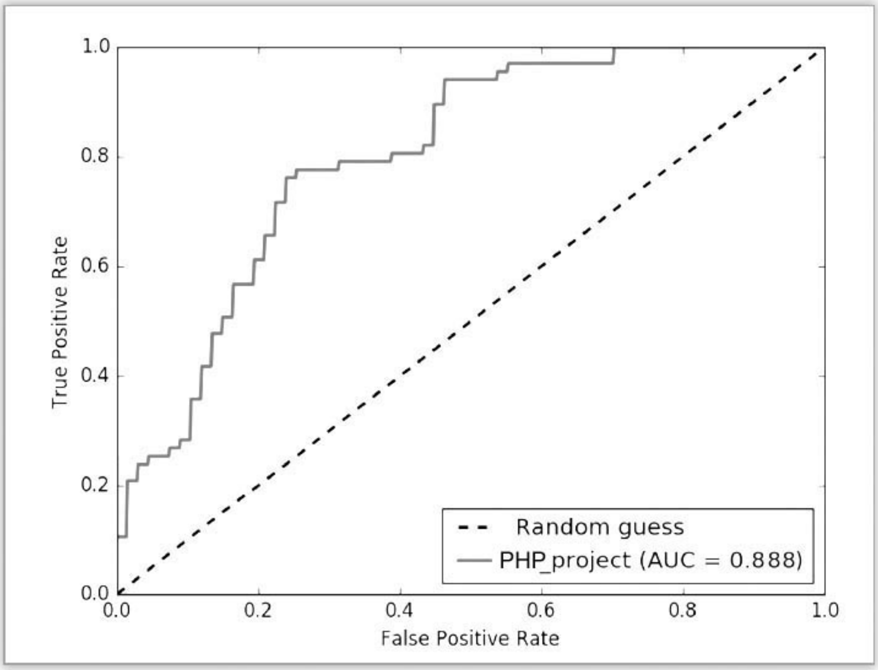

Figure 24. ROC curve—PHP.

The generated curve displays the area under the curve (AUC). The AUC represents the degree or measure of separability achieved by the model. It quantifies the overall ability of the model to discriminate between positive and negative classes. AUC values range from 0 to 1. For AUC = 1, we have a perfect model that correctly classifies all positive and negative cases. For AUC = 0.5, we have a model with no discriminative ability, equivalent to a random guess. For AUC < 0.5, we have a model that performs worse than random guessing, indicating a poor classifier.

The reliability of the cumulative geohazard map has been tested using the ROC method in the QGIS environment with the SZ plugin, which is an open source tool. Feature points were selected across the PHP area, in each landscape character zone, of selective cumulative geohazard zones, which were verified by field survey. ROC analysis yielded an AUC with a value of 0.888. The final result demonstrates a highly satisfactory operation of the GPI [43,63].

3.4. Spatial Identifications for Geohazard Prevention

The final zoned cumulative geohazard map provides the means to spatially identify critical sub-zones and the locations of heritage features within them (Figure 25). The delineation and identification of these entities was achieved by combining the geohazard prevention zones with the landscape character zones. This was carried out by assigning to each sub-zone both the landscape character with its heritage features and the significance of the cumulative geohazard that threatens it. The dual identity of the sub-zones, as well as their content, provide indications for early prevention with targeted actions. These indications answer the question of what is likely to happen and where it is going to happen, with the objective of reducing or preventing such occurrences.

The results demonstrate the capacity of the tool to identify spatial units of varying graded geohazards. The geohazard zones in the PHP that are potentially most endangered are presented in more detail below.

As evidenced by the case of the Framework application in the PHP, sub-zones of considerable geohazard importance are observed over a vast area in landscape character zone Mt. Tetrazion, as well as in a limited area in the Mt. Lykaion LCZ. Sub-zones of notable importance are distributed across a significant portion of the Mt. Tetrazion LCZ, Mt. Lykaion LCZ, and Neda LCZ. It is also observed that heritage features are included in or are close to these sub-zones. It is crucial to note the importance of the heritage features contained in each sub-zone, as well as the size of the area it covers. It should also be stressed that they are not always observed in proportion. For example, there may be few valuable features that need prevention in a large spatial coverage of high geohazards. Indicative sub-zones are pictured in black polygons in Figure 25.

In the Mt. Tetrazio LCZ, located to the south of the villages of Isari and Vasta and to the east of the sanctuary and temple at Melpia, the cumulative geohazard is classified as grade 6 to 7 (on a ten-point scale, as previously outlined in the text). In the same LCZ, to the east of the ancient city of Trapezous, a geohazard zone of grade 6 is observed.

In the Neda LCZ, specifically in the area of Vasses and to the south of Linistaina village on the Neda tributary, the geohazard index reaches grade 6. In the village of Kakaletri, situated in close proximity to the ancient town of Eira, the geohazard index has been determined to be at grade 6. Additionally, a grade 6 index is observed in the region south of Figalia and the temple of Athena and Zeus in Figalia.

In areas where geohazard grades 6 and 7 (slightly high and/or high) are prevalent, there is an urgent need for further in situ studies. As can be observed, the intensifying phenomena of climate change are resulting in a reduction in overall rainfall but an increase in the intensity of precipitation events. The occurrence of high rainfall rates in a relatively short period of time, coupled with the presence of prolonged periods of high temperatures (i.e., during drought conditions), can lead to an increase in geohazards, such as weathering and erosion. This, in turn, can result in the occurrence of landslides and subsidence, which can further magnify the observed phenomenon.

In the specific context of the area of interest, the contribution of each geohazard to the cumulative geohazard is as follows: 36.5% landslide, 5.1% earthquake, 9.2% weathering, 23.5% erosion, and 25.7% sedimentation. These figures are based on the given climatic conditions (summer with variable rainfall) and the existing state of the natural environmental factors.

Consequently, in order to ascertain the relationship between geohazards and landscapes containing sensitive features of cultural and natural heritage, it is necessary to implement a focused planning strategy involving comprehensive surveys and in situ studies, with the objective of achieving sustainable management [64–66].

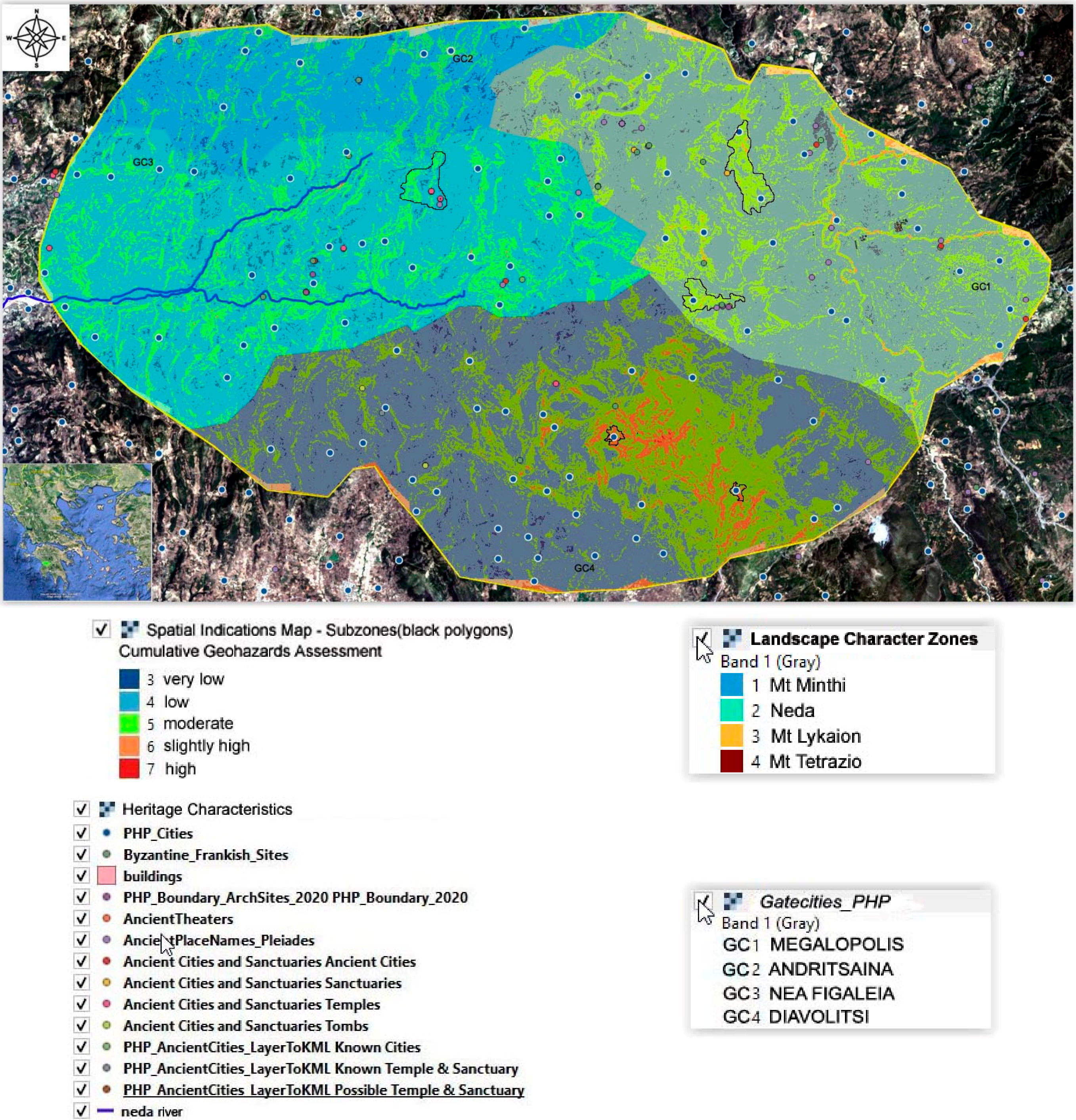

Figure 25. Spatial identification map for geohazard prevention.

4. Discussion

The proposed methodological framework places significant emphasis on the importance of prevention, thus the pre-management stage of cultural and natural heritage areas. In these areas, the environmental factors that contribute to the occurrence of geohazards assume a distinct role with respect to the protection of their heritage features, compared to the factors and geohazards present in other areas. Hence, the framework is specifically designed to facilitate early prevention by taking into account the factors and their degree of involvement in the development of geohazards. The framework is based on a cumulative approach to geohazard assessment and considers not only the individual geohazards present in the area but also the collective impact of all geohazards on the cultural and natural heritage landscape.

Previous research internationally has mainly dealt with the assessment of one geohazard at a time, mainly concerning landslides and earthquakes. There is no specific focus on cultural and natural heritage sites, which have sensitive heritage features that require timely and detailed investigation for their protection.

A limitation of focusing on a single geohazard is that it fails to consider the full range of potential geohazards, which may result in an incomplete understanding of the impacts posed by geologic phenomena. This approach presents a number of significant disadvantages. It may result in the inadvertent overlooking of other potential threats. For instance, in the context of earthquake preparedness, the one-hazard approach may neglect to consider the potential risks associated with landslides. Conversely, this approach may result in an erroneous assumption of protection. It is evident that areas of cultural and natural heritage are susceptible to a multitude of geohazards that have yet to be assessed. It is conceivable that the implementation of mitigation measures for one geohazard may not address and could even exacerbate the risks associated with other geohazards. Moreover, there is an increased vulnerability and a lack of comprehensive preparedness. A narrow focus on a single geohazard may result in an incomplete understanding of the potential for that geohazard to trigger another. Heavy precipitation can precipitate landslides, which may not be considered if the study in question focuses exclusively on rainfall. In general, the protection of a heritage landscape through the study of a single geohazard can result in significant vulnerabilities, an inefficient use of resources, and an inadequate preparedness and response strategy.

Thus, it is apparent that a cumulative geohazard approach is indispensable for the prevention and preservation of the heritage landscape. The principal advantages of a cumulative approach include a more comprehensive understanding of preparedness, improved mitigation, enhanced decision-making, increased awareness, and long-term sustainability. In the context of climate change, cumulative assessments are of particular importance, as they can identify how changing environmental conditions may influence the frequency and severity of geohazards. This approach encourages interdisciplinary collaboration, facilitating the development of innovative solutions and enhanced predictive models. The application of advanced technologies, including geographic information systems (GIS), remote sensing, and big data analytics, can enhance the accuracy and comprehensiveness of cumulative geohazard assessments.

Therefore, the cumulative approach to geohazard assessment facilitates a more comprehensive understanding of the upcoming threats, ultimately contributing to the protection of heritage landscapes and their resilient communities.

5. Conclusions

The findings of the research indicate that by utilizing the proposed methodological framework and the GPI in accordance with their intended specifications, critical questions can be answered. These include whether the framework is a prevention tool, whether it is usable, whether it is technologically up to date, whether it is economical to use, whether it provides spatial information, and finally, whether it is effective.

The process is one of reconnaissance, which enables the timely anticipation of the evolution of cumulative geohazards. The implementation of the methodological framework is subject to the specific conditions of the natural environment in the area of interest. Furthermore, it may be applied on a daily basis in instances where intensifying phenomena are observed in the area as an impact of climate change. The framework's index is designed to accommodate the distinctive characteristics of each region. The prevention framework is a useful and rapid tool that operates in a modern technological environment. It is based on spatial analysis and requires no cost to operate, utilizing digital information and techniques. Its utility lies in the capacity to early inform decision-making processes regarding effective and responsible environmental management.

The contribution of this research is evident in the creation of such a methodological framework for geohazard prevention, which introduces a new index for assessing geohazards that threaten heritage landscapes. These landscapes are more sensitive and therefore require special attention and preparedness to reduce the impact of geohazards. The structure of the index is based on an innovative approach—the cumulative approach. It emphasizes the spatial dimension by using new technologies and working in a GIS environment. The index provides the opportunity to identify the most significant environmental factors associated with geohazards and the relationships between all geohazards. It also allows for the comprehension of the contribution of multiple parameters to the genesis of geohazards and the interpretation of the generation mechanisms and processes of their occurrence. This is accomplished by employing data investigations, analytical processes, and the interpretation of the acquired information pertinent to the specific area.

As previously indicated, the framework and the index are intended for application to terrestrial cultural and natural heritage areas. Hence, a future research development would be an analysis of geohazards and their environmental factors in heritage areas affected by the sea. Subsequently, the index will be expanded to include new terms and weights. It should be noted that the framework and its index cannot be applied to any area; they address the assessment of geohazards in cultural and natural heritage landscapes.

As this tool will contribute to the sustainable management of these areas, the implications of its utilization can be summarized as follows: It indicates spatial designations for actions to mitigate or even prevent the evolution of geohazards, which by their very nature require local studies. Subsequently, the tool addresses the conservation of valuable and sensitive landscapes and their features, with the objective of enhancing them where necessary. Ultimately, this tool facilitates the reduction in time and financial expenditure associated with unnecessary and costly actions, thereby advancing the sustainable management of cultural and natural heritage landscapes.

Overall, this geohazard assessment approach serves to highlight the necessity of acquiring the requisite knowledge to adopt preventive measures and site-specific mitigation strategies in a timely manner, thereby preventing the acceleration of geohazards into disasters. Furthermore, it serves to highlight the necessity of protecting landscapes with cultural and natural heritage characteristics for future generations.

Author Contributions: Conceptualization, G.F.D.P.; Methodology, G.F.D.P. and M.P.P.; Validation, G.F.D.P. and M.P.P.; Formal analysis, G.F.D.P.; Investigation, G.F.D.P.; Resources, G.F.D.P.; Data curation, G.F.D.P.; Writing—original draft, G.F.D.P.; Writing—review & editing, M.P.P.; Visualization, G.F.D.P.; Supervision, M.P.P.; Project administration, M.P.P. All authors have read and agreed to the published version of the manuscript.

Funding: This research received no external funding.

Data Availability Statement: The original contributions presented in the study are included in the article, further inquiries can be directed to the corresponding author.

Conflicts of Interest: The authors declare no conflicts of interest.

Appendix A

Information on the data source and the GIS data type:

- Landsat 8 satellite image (Source: USGS)
- Digital terrain model (Data type: raster layer)
- Lithology data (Source: Hellenic Geological and Mineral Exploration Authority, Data type: vector layer)

- Faults data (Source: Hellenic Geological and Mineral Exploration Authority, Data type: vector layer)
- Land use data (Source: Copernicus, Data type: vector layer)
- Rainfall data (Source: Hellenic National Meteorological Service, Data type: vector layer)
- Surface water data (Source: geodata.gov.gr, Data type: vector layer)
- Groundwater data (Source: geodata.gov.gr, Data type: vector layer)
- Road Network data (Source: geodata.gov.gr, Data type: vector layer)
- Peak Ground Accelerator data (Source: GreDaSS, Data type: vector layer)
- Cultural characteristics (Source: National Monuments Archive, 2023, Ministry of Culture, vector layer).

References

1. UNESCO. Convention Concerning the Protection of the World Cultural and Natural Heritage. Statement of Outstanding Universal Value, 37 COM 8E Paris 2013, France. Available online: https://whc.unesco.org/archive/2013/whc13-37com-8e-en.pdf (accessed on 27 June 2024).
2. Thomson, J.; Regan, T.; Hollings, T.; Amos, N.; Geary, W.; Parkes, D.; Hauser, C.; White, M. Spatial conservation action planning in heterogeneous landscapes. *Biol. Conserv.* **2020**, *250*, 108735. [CrossRef]
3. Hersperger, A.; Bürgi, M.; Wende, W.; Bacău, S.; Grădinaru, S. Does landscape play a role in strategic spatial planning of European urban regions? *Landsc. Urban Plan.* **2020**, *194*, 103702. [CrossRef]
4. Council of Europe. Cultural Heritage, Landscape and Spatial Planning Division, 2000, "European Landscape Convention and Reference Documents", Directorate of Culture and Cultural and Natural, F-67075 STRASBOURG Cedex France. Available online: https://rm.coe.int/european-landscape-convention-book-text-feb-2008-en/16802f80c6 (accessed on 27 June 2024).
5. Papakonstantinou, G.F.; Papadopoulou, M. Establishing Cultural and Natural Heritage Areas as Protected Landscapes: An Institutional Framework in Greece. Special Theme Issue, Planning in Transition: The Case of Greece. *Plan. Pract. Res.* 2024, *in press*. [CrossRef]
6. Davis, G.; Kranis, H. The Parrhasian Park Viewed in Geologic Perspective. In Proceedings of the Scientific Conference "Protecting and Promoting the Values of the Cultural and Natural Environment in the Areas Where Arcadia, Messenia, and Elis Meet", Athens, Greece, 31 May 2019.
7. UNESCO. Paris, 26 November 2020, Addressing Climate Change Impacts on Cultural and Natural Heritage. Available online: https://unesdoc.unesco.org/ark:/48223/pf0000374569 (accessed on 27 June 2024).
8. Papakonstantinou, G.F.; Papadopoulou, M.P. The geological process, a generating cause of Heritage in the mountainous area of Parrhasian Park of the Peloponnese. In Proceedings of the 10th Congress, National Technical University of Athens (NTUA) and Metsovion Interdisciplinary Research Center (MIRC), Metsovon, Greece, 22–24 September 2022.
9. ICOMOS. The New Triennial Scientific Plan 2021–2024—Cultural Heritage and Climate Action 2021. Available online: https://www.icomos.org/en/focus/climate-change/104837-adoption-of-the-new-triennial-scientific-plan-2021-2024-cultural-heritage-and-climate-action (accessed on 27 June 2024).
10. Kapsomenakis, J.; Douvis, C.; Poupkou, A.; Zerefos, S.; Solomos, S.; Stavraka, T.; Melis, N.S.; Kyriakidis, E.; Kremlis, G.; Zerefos, C. Climate change threats to cultural and natural heritage UNESCO sites in the Mediterranean. *Environ. Dev. Sustain.* **2023**, *25*, 14519–14544. [CrossRef]
11. Address by Mechtild Rössler, on the Protection of European Cultural Heritage from Geo-Hazards (PROTHEGO) Project: European World Heritage Sites Affected by Geo-Hazards, Satellite Monitoring Future Challenges; UNESCO HQ, 23 March 2018. Available online: https://unesdoc.unesco.org/ark:/48223/pf0000261795 (accessed on 27 June 2024).
12. Mavroulis, S.; Diakakis, M.; Kranis, H.; Vassilakis, E.; Kapetanidis, V.; Spingos, I.; Kaviris, G.; Skourtsos, E.; Voulgaris, N.; Lekkas, E. Inventory of Historical and Recent Earthquake-Triggered Landslides and Assessment of Related Susceptibility by GIS-Based Analytic Hierarchy Process: The Case of Cephalonia (Ionian Islands, Western Greece). *Appl. Sci. Spec. Issue Mapp. Monit. Assess. Disasters* **2022**, *12*, 2895. [CrossRef]
13. Hutchinson, J.N. General report morphological and geotechnical parameters of landslides in relation to geology and hydrogeology. In Proceedings of the 5th International Symposium on Landslides, Lausanne, Switzerland, 10–15 July 1988.
14. Van Westen, C.J.; Van Asch, T.W. Landslide hazard and risk zonation—Why is it still so difficult? *Bull. Eng. Geol. Environ.* **2006**, *65*, 167–184. [CrossRef]
15. Dai, F.C.; Lee, C.F.; Ngai, Y.Y. Landslide risk assessment and management: An overview. *Eng. Geol.* **2002**, *64*, 65–87. [CrossRef]
16. Burton, P.; Yebang, X.; Tselentis, A.; Sokos, E.; Aspinall, W. Strong ground acceleration seismic hazard in Greece and neighboring regions. *Soil Dyn. Earthq. Eng.* **2003**, *23*, 159–181. [CrossRef]
17. Agapiou, A. UNESCO World Heritage properties in changing and dynamic environments: Change detection methods using optical and radar satellite data. *Herit. Sci.* **2021**, *9*, 64. [CrossRef]
18. Cruden, D.M.; Varnes, D.J. Landslide types and processes. U.S. National Academy of Sciences, Special Report. *Transp. Res. Board* **1996**, *247*, 36–75.
19. Dai, F.C.; Lee, C.F. Landslide characteristics and slope instability modeling using GIS. *Geomorphology* **2002**, *42*, 213–228. [CrossRef]

20. Lee, S.; Ryu, J.H.; Min, K.; Won, J.S. Landslide susceptibility analysis using GIS and artificial neural network. *Earth Surf. Process. Landf.* **2003**, *28*, 1361–1376. [CrossRef]
21. Ohlmacher, G.C.; Davis, J.C. Using multiple logistic regression and GIS technology to predict landslide hazard in northeast Kansas, USA. *Eng. Geol.* **2003**, *69*, 331–343. [CrossRef]
22. Guzzetti, F.; Carrara, A.; Cardinali, M.; Reichenbach, P. Landslide hazard evaluation: A review of current techniques and their application in a multi-scale study, Central Italy. *Geomorphology* **1999**, *31*, 181–216. [CrossRef]
23. Guzzetti, F.; Peruccacci, S.; Rossi, M.; Stark, C.P. Rainfall thresholds for the initiation of landslides in central and southern Europe. *Meteorol. Atmos. Phys.* **2007**, *98*, 239–267. [CrossRef]
24. Montgomery, D.R.; Dietrich, W.E. A physically based model for the topographic control on shallow landsliding. *Water Resour. Res.* **1994**, *30*, 1153–1171. [CrossRef]
25. Tilling, R.I.; Dvorak, J.J. Volcanoes in Human History. In *Overview of Volcanic Hazards*; Princeton University Press: Princeton, NJ, USA, 1993; pp. 11–30.
26. Stein, R.S.; Wysession, M. *An Introduction to Seismology, Earthquakes, and Earth Structure*; Wiley-Blackwell: Hoboken, NJ, USA, 1991; ISBN 978-0-865-42078-6.
27. Boore, D.M.; Joyner, W.B.; Fumal, T.E. Equations for estimating horizontal response spectra and peak acceleration from western North American earthquakes: A summary of recent work. *Seismol. Res. Lett.* **1997**, *68*, 128–153. [CrossRef]
28. White, A.F.; Brantley, S.L. The effect of time on the weathering of silicate minerals: Why do weathering rates differ in the laboratory and field? *Chem. Geol.* **2003**, *202*, 479–506. [CrossRef]
29. Fitzpatrick, E.A.; Knox, J.C.; Seidl, M.A. Soil weathering rates and drainage basin morphology in the Driftless Area, Wisconsin and Illinois, USA. *Geomorphology* **1999**, *29*, 315–327.
30. Dixon, J.L.; Turkington, A.V. Dynamic relationship between soil erosion, vegetation cover and topography in a semi-arid ecosystem. *Earth Surf. Process. Landf. J. Br. Geomorphol. Res. Group* **2006**, *31*, 1344–1360.
31. Foster, G.R.; Meyer, L.D. A closed-form equation for predicting the hydraulic conductivity of unsaturated soils. *Soil Sci. Soc. Am. J.* **1972**, *36*, 445–449.
32. Schumm, S.A. *The Fluvial System*; Wiley: New York, NY, USA, 1977.
33. Gomi, T.; Sidle, R.C.; Richardson, J.S. Understanding processes and downstream linkages of headwater systems. *BioScience* **2002**, *52*, 905–916. [CrossRef]
34. Ferrara, V.; Miccadei, E.; Ponzo, F.C. Subsidence and groundwater withdrawal in Venice. *Environ. Geol.* **2011**, *60*, 389–398.
35. Dai, H.; Lei, G. Study on land subsidence caused by over-extraction of groundwater based on time-series InSAR technology: A case study of Wuhan, China. *Water* **2019**, *11*, 1091.
36. Tsai, F.; Liu, C.; Hsieh, C. Land subsidence induced by groundwater pumping and geological conditions in the Choushui River alluvial fan, Taiwan. *Eng. Geol.* **2016**, *202*, 121–130.
37. Teatini, P.; Tosi, L.; Strozzi, T. Twenty years of land subsidence in Venice studied by spatial interferometry. *Eng. Geol.* **2005**, *79*, 267–297.
38. Pavlickova, K.; Vyskupova, M. A method proposal for cumulative environmental impact assessment based on the landscape vulnerability evaluation. *Environ. Impact Assess. Rev.* **2015**, *50*, 74–84. [CrossRef]
39. Christian, J.; Baecher, G.D.W. Taylor and the Fundamentals of Soil Mechanics. *Geotech. Geoenvironmental Eng.* **2015**, *141*, 02514001. [CrossRef]
40. Saaty, T.L. *The Analytic Hierarchy Process*; McGraw-Hill: New York, NY, USA, 1980.
41. Nandi, A.; Shakoor, A. A GIS-based landslide susceptibility evaluation using bivariate and multivariate statistical analyses. *Eng. Geol.* **2010**, *110*, 11–20. [CrossRef]
42. Jenks, G.F. Generalization in Statistical Mapping. *Ann. Assoc. Am. Geogr.* **1963**, *53*, 15–26. [CrossRef]
43. Fawcett, T. An introduction to ROC analysis. *Pattern Recognit. Lett.* **2006**, *27*, 861–874. [CrossRef]
44. Davison, M. A New Era of National Heritage Parks: Building Resilient Communities, Conserving Nature and Retaining Heritage. In Proceedings of the Scientific Conference "Protecting and Promoting the Values of the Cultural and Natural Environment in the Areas where Arcadia, Messenia, and Elis Meet", Athens, Greece, 31 May 2019.
45. Romano, D.G.; Voyatzis, M.E. Mt. Lykaion Excavation and Survey Project, Part 2, The Lower Sanctuary. *Hesperia* **2015**, *84*, 264–266.
46. Romano, D.G. The Idea of the Parrhasian Heritage Park. In Proceedings of the Scientific Conference "Protecting and Promoting the Values of the Cultural and Natural Environment in the Areas where Arcadia, Messenia, and Elis Meet", Athens, Greece, 31 May 2019.
47. Available online: https://www.parrhasianheritagepark.org/ (accessed on 5 August 2024).
48. Martine, B.-D.; Luginbühl, Y.; Terrasson, D. *Landscape, from Knowledge to Action*; Editions Quae: Versailles, France, 2008; pp. 168–183.
49. Wascher, D.M. (Ed.) *European Landscape Character Areas—Typologies, Cartography and Indicators for the Assessment of Sustainable Landscapes*; Landscape Europe: Wageningen, The Netherlands, 2005.
50. Reyes, V. The production of cultural and natural wealth: An examination of World Heritage sites. *Poetics* **2014**, *44*, 42–63. [CrossRef]
51. Brückner, H.; Kelterbaum, D.; Marunchak, O.; Porotov, A.; Vott, A. The Holocene sea level story since 7500 BP—Lessons from the Eastern Mediterranean, the Black and the Azov Seas. *Quat. Int.* **2010**, *225*, 160–179. [CrossRef]

52. Available online: https://www.parrhasianheritagepark.org/documents/73/MTL_2023_Report_of_Activities_FINAL.pdf (accessed on 5 August 2024).
53. Available online: https://www.parrhasianheritagepark.org/park-planning1/ (accessed on 5 August 2024).
54. Available online: https://www.ascsa.edu.gr/events/details/protecting-and-promoting-the-values-of-the-cultural-and-natural-environment-in-the-areas-where-arcadia-messinia-and-elis-meet (accessed on 5 August 2024).
55. Polunin, O. *Flowers of Greece and the Balkans. A Field Guide*; Oxford University Press: Oxford, UK, 1987.
56. Harvati, K.; University of Tübingen. European Project "Human Evolution at the Crossroads". Available online: https://cordis.europa.eu/project/id/724703 (accessed on 27 June 2024).
57. Papadopoulos, G.A.; Baskoutas, I.; Fokaefs, A. Historical seismicity of the Kyparissiakos Gulf, western Peloponnese, Greece. *Boll. Di Geofis. Teor. Ed Appl.* **2014**, *55*, 389–404.
58. Vött, A. Relative sea level changes and regional tectonic evolution of seven coastal areas in NW Greece since the mid-Holocene. *Quat. Sci. Rev.* **2007**, *26*, 894–919. [CrossRef]
59. Bald, I.; Davis, G.; Romano, D.G. The Monument Landscape and Associated Geology at the Sanctuary of Zeus on Mt. Lykaion. In *Asmosia X Digital Version*; «L'ERMA» di Bretschneider Publishing House: Rome, Italy, 2015; pp. 429–436.
60. Davis, G. Geology of the Sanctuary of Zeus, Mount Lykaion, Southern Peloponessos, Greece, and Field Guide. *J. Virtual Explor. Electron. Ed.* **2019**, *33*, 58. [CrossRef]
61. Reed, R.W.; Kassawara, R.P. A criterion for determining exceedance of the operating basis earthquake. *Nucl. Eng. Des.* **1990**, *123*, 387–396. [CrossRef]
62. Greek Database of Seismogenic Sources. Available online: https://gredass.unife.it/ (accessed on 27 June 2024).
63. Titti, G.; Sarretta, A.; Lombardo, L.; Crema, S.; Pasuto, A.; Borgatti, L. Mapping Susceptibility With Open-Source Tools: A New Plugin for QGIS. *Front. Earth Sci.* **2022**, *10*, 842425. [CrossRef]
64. Venkatachalam, T.; Day, J.; Heron, S. A systematic approach for defining thematic groups of World Heritage properties to support the strategic management of threats. *Environ. Chall.* **2022**, *8*, 100538. [CrossRef]
65. De Beer, J.; Boogaard, F. Good practices in cultural heritage management and the use of subsurface knowledge in urban areas. *Procedia Eng.* **2017**, *209*, 34–41. [CrossRef]
66. Durrant, L.; Vadher, A.; Teller, J. Disaster risk management and cultural heritage: The perceptions of European world heritage site managers on disaster risk management. *Int. J. Disaster Risk Reduct.* **2023**, *89*, 103625. [CrossRef]

Disclaimer/Publisher's Note: The statements, opinions and data contained in all publications are solely those of the individual author(s) and contributor(s) and not of MDPI and/or the editor(s). MDPI and/or the editor(s) disclaim responsibility for any injury to people or property resulting from any ideas, methods, instructions or products referred to in the content.